68

Measurement and Formulation of the Thermodynamic Properties of Refrigerants 134a (1,1,1,2-Tetrafluoroethane) and 123 (1,1-Dichloro-2,2,2-Trifluoroethane)

M.O. McLinden, Ph.D. *Associate Member ASHRAE*
J.S. Gallagher
L.A. Weber, Ph.D.
G. Morrison, Ph.D.
D. Ward
A.R.H. Goodwin, Ph.D.
M.R. Moldover, Ph.D.
J.W. Schmidt, Ph.D.
H.B. Chae, Ph.D.
T.J. Bruno, Ph.D.
J.F. Ely, Ph.D.
M.L. Huber, Ph.D.

ABSTRACT

The thermodynamic properties of R134a and R123 are formulated using a modified Benedict-Webb-Rubin (MBWR) equation of state fit to experimental measurements of the critical point, vapor pressure, saturated liquid and vapor volumes, superheated pressure-volume-temperature (p-V-T) behavior, and second virial coefficients derived from p-V-T and sound speed measurements. The heat capacity of the ideal gas reference state is determined from sound speed measurements on the low density vapor. Surface tensions are also presented. The experimental methods and results are summarized, compared to the property formulation and, where possible, compared to other sources in the literature. Tables and diagrams of the thermodynamic properties of R134a and R123, prepared using the MBWR equation of state, are presented. While the various measurements cover different ranges of temperature and pressure, the MBWR formulation is applicable in both the liquid and vapor phases at pressures up to 10,000 kPa (1500 psia); the applicable temperature range is 233 to 450 K (−40° to 350°F) for R134a and 255 to 450 K (0° to 350°F) for R123.

INTRODUCTION

The advent of the Montreal Protocol restricting the future production of certain fully halogenated chlorofluorocarbon (CFC) refrigerants and more recent calls from many quarters to completely or nearly completely ban their production present a major challenge to the refrigeration industry. There are a number of very promising fluids that may serve as substitutes, either as pure fluids, as constituents of mixtures, or both. In particular R134a (CF_3CFH_2) and R123 (CCl_2HCF_3) have emerged as leading candidates to replace R12 and R11, respectively. They are under active worldwide development by a number of chemical manufacturers working with the refrigeration and air-conditioning industry.

In order to evaluate the performance (energy efficiency, capacity, etc.) of these or any other replacement working fluids in heat pumping, air-conditioning, or refrigerating applications, a complete set of thermodynamic properties is required. Development efforts by equipment manufacturers have been hampered by property data that are sparse, conflicting, proprietary or, in some cases, simply unavailable (Hickman 1988). The situation with R134a has been considerably improved by the recent publication of measurements by Wilson and Basu (1988) and Kabata et al. (1988). The data for R123, however, remain very sparse, at least in the open literature. Even for R134a, values listed on property summary sheets prepared by various chemical manufacturers are often inconsistent.

The objectives of the present project are to measure for R134a and R123 the basic data necessary to define the thermodynamic surface, to fit these data, along with other data available in the literature, to an equation of state, and

M.O. McLinden, T.J. Bruno, and **M.L. Huber** are chemical engineers and **J.F. Ely** is a group leader in the Thermophysics Division, National Institute of Standards and Technology, Boulder, CO; **J.S. Gallagher, L.A. Weber,** and **J.W. Schmidt** are physicists, **G. Morrison** is a research chemist, **A.R.H. Goodwin** and **H.B. Chae** are guest workers, and **M.R. Moldover** is a group leader in the Thermophysics Division and **D. Ward** is an engineering technician in the Building Environment Division, NIST, Gaithersburg, MD.

to use this equation of state to generate tables and diagrams of the thermodynamic properties. This paper will focus on the last two aspects—fitting the data and presenting them in a convenient and usable form. The measurement techniques themselves and the rationale behind them will be outlined, but the full details, including the actual experimental data, will be presented elsewhere (e.g., Chae et al. 1989; Goodwin and Moldover 1989; Weber 1989; Morrison and Ward 1989; Weber and Levelt-Sengers 1989). Any property formulation is merely a correlation of the actual thermodynamic behavior of a fluid and is therefore subject to change as additional experimental or theoretical information becomes available. The property formulations to be presented here are felt to represent the actual thermodynamic properties of these fluids as well as possible given the present data; while fully adequate for engineering calculations, they must, however, be considered provisional. A final formulation of properties must await more extensive measurements, which should be under way by the time this report is published.

REQUIREMENTS FOR THE DEFINITION OF THE THERMODYNAMIC SURFACE

For calculations involving thermodynamic properties, one rarely has a collection of experimental data that is sufficiently large to permit interpolation at all points of interest. Instead one employs an equation of state. An equation of state is a function that can correlate all the thermodynamic properties of a fluid in a consistent way. Furthermore, it is a fundamental relationship from which all the thermodynamic properties of a material can be derived by applying the appropriate thermodynamic operations. An equation of state thus allows the calculation of quantities, such as entropy, that may not have been, or cannot be, directly measured.

An equation of state typically expresses the pressure, p, as a function of absolute temperature, T, molar volume, V, and a set of adjustable parameters, a_i:

$$p = f(T, V, a_i) \tag{1}$$

Other thermodynamic quantities are obtained by manipulation of Equation 1. Integration of Equation 1 over volume yields the Helmholtz free energy:

$$A = -\int p\, dV \tag{2}$$

Care must be taken in choosing the limits of this integration; the most convenient choice for the upper limit is $V = \infty$, where all gases follow the ideal gas law:

$$p = RT/V \tag{3}$$

In the limit of $V = \infty$, however, the integral of pdV diverges; this problem is avoided by integrating over the difference between the actual pressure as given by Equation 1 and the pressure of the ideal gas reference state (Equation 3) to obtain the difference between the actual Helmholtz free energy, A, and that of the reference state, A^0:

$$A(V,T) - A^0(V,T) = \int_v^\infty (p - RT/V)\, dv \tag{4}$$

Once the Helmholtz free energy is evaluated, the other thermodynamic functions follow. Entropy is given by

$$S = -\left[\frac{\partial A}{\partial T}\right]_v \tag{5}$$

so that the difference between S and the reference state entropy is given by the derivative of Equation 4:

$$S - S^0 = -\left[\frac{\partial}{\partial T}(A - A^0)\right]_v \tag{6}$$

The results of the integration in Equation 4 and the differentiation in Equation 6 represent only the volume dependence of A and S. The temperature dependence of these quantities is contained in the ideal gas reference state; for entropy:

$$S^0 = S_{ref} + \int_{T_{ref}}^{T} C_p^0/T\, dT \tag{7}$$

where T_{ref} is an arbitrary reference temperature at which entropy is set to an arbitrary reference value, S_{ref}; a common choice for refrigerants is $S_{ref} = 0$ at $T_{ref} = 233.15$ K (−40°F). Thus, in addition to an equation of state (e.g., Equation 1) a second fundamental requirement to define the thermodynamic behavior of a fluid is knowledge of C_p^0, the heat capacity of the vapor in the limit of zero pressure. (Other reference states, which, in turn, would require calorimetric information other than C_p^0, can be defined. The choice of the ideal gas reference state and the resulting need for C_p^0 information is the most convenient from both numerical and experimental viewpoints.)

The other thermodynamic quantities arise by similar operations. As examples:

$$H = A + TS + pV \tag{8}$$

$$H - H^0 = (A - A^0) + T(S - S^0) + (pV - RT) \tag{9}$$

$$C_v = T\left[\frac{\partial S}{\partial T}\right]_v \tag{10}$$

$$C_v - C_v^0 = T\left[\frac{\partial}{\partial T}(S - S^0)\right]_v \tag{11}$$

$$C_v^0 = C_p^0 - R \tag{12}$$

$$C_p = C_v - T\left[\frac{\partial p}{\partial T}\right]_v^2 \Big/ \left[\frac{\partial p}{\partial V}\right]_T \tag{13}$$

The saturation pressure (vapor pressure) is obtained from an equation of state by the equality of pressures and by use of the criteria for phase equilibria:

$$G(T, V_l) = G(T, V_v) \tag{14}$$

where G, the Gibbs free energy, is evaluated for the specific volumes of the liquid and vapor phases, V_l and V_v. G is given by

$$G - G^0 = (A - A^0) + (pV - RT) \tag{15}$$

An equation of state, along with information on the ideal gas heat capacity, thus ties together all the thermodynamic properties of a fluid. Which properties to measure in order to define a fluid is dictated more by the form of the equation of state and the accuracy and ease with which one can measure various quantities than by which quantities are required for a particular application, such as the calculation of cycle efficiency. The measurements carried out in this work consist of pressure-volume-temperature (p-V-T) measurements along lines of constant volume in the vapor phase, saturated liquid density and vapor pressure over a range of temperature, and a determination of the critical point parameters. These data represent the minimum information necessary to define an equation of state covering the range of temperature and pressure of interest for refrigeration applications. Other approaches, built around other data sets, are possible; the approach taken here and its associated data set are the most common. The ideal gas heat capacity, C_p^0, is derived from measurements of the speed of sound in the low pressure vapor. In addition, the surface tension of R134a and R123 was determined by the capillary rise method.

SYNOPSIS OF EXPERIMENTS

p-V-T Measurements

The most important data for characterizing the thermodynamic properties of a fluid in the single-phase region are measurements of the pressure-volume-temperature behavior. In this work, measurements were carried out on an apparatus operating in distinct Burnett and isochoric modes as described by Linsky et al. (1987). The fluid sample is contained in a heavy-walled metal vessel having two chambers of volumes, V_1 and V_2, separated by a valve. The sample vessel is submerged in a circulating oil bath whose temperature is maintained within 1 mK (0.002°F) of the desired value. Thermal variations within the bath are less than 2 mK (0.004°F). Pressures are measured with either a quartz Bourdon gauge (accurate to 0.2kPa [0.03 psia]) with digital readout or a manually operated gas dead-weight gauge accurate to ±0.002 kPa [±0.03 psia]). The argon used in the pressure lines is separated from the fluid sample by a nickel diaphragm transducer, located in the oil bath, which is sensitive to 0.01 kPa (0.0015 psia).

The specific volume (or density) of the sample is determined indirectly by the Burnett (1936) method. This method avoids the difficult determination of the cell volume and sample mass. In the Burnett mode of operation, data are measured at a constant temperature by filling the first chamber, V_1, to the maximum desired pressure and density and evacuating V_2. After measuring the initial pressure, p_0, the valve connecting V_1 and V_2 is opened and the sample fills both chambers at a lower pressure, p_1. The valve is closed, V_2 is again evacuated, and the process is repeated, measuring p_2, p_3, etc., until the minimum pressure that can be accurately measured is reached. The ratio between the total volume and that of V_1 defines the volume ratio:

$$N_i = \frac{Y_1(p_i) + Y_2(p_i)}{Y_1(p_{i-1})} \tag{16}$$

Usually the volume ratio is chosen to have a value between 1.5 and 2 (1.78 in our case); it is a very weak function of pressure as indicated by the p's in Equation 16. The volume ratio, including its pressure dependence, was determined in a separate experiment by a calibration with helium.

The specific volume of the sample in successive expansions follows from the definition of the volume ratio:

$$V_i = V_{i-1} N_i \tag{17}$$

The volume for any given expansion can then be expressed as:

$$V_i = V_0 \prod_{j=1}^{i} N_j \tag{18}$$

where V_0 is the initial molar volume of the sample and $\prod N_j$ is the product of the N's. The molar volume can be related to the pressure through the use of the compressibility factor, $Z = pV/RT$:

$$p_i = \frac{RTZ_i}{V_0 \prod_{j=1}^{i} N_j} \tag{19}$$

The above equations lead to an undetermined problem—there are more unknowns (V_i, Z) than equations. The situation can be resolved by defining the compressibility factor in terms of a finite virial expansion:

$$Z = 1 + B/V + C/V^2 + D/V^3 \tag{20}$$

where B, C, and D are the second, third, and fourth virial coefficients and are functions only of temperature. This yields one equation for each measured pressure:

$$p_i = \frac{RT}{V_0 \prod_{j=1}^{i} N_j}\left[1 + \frac{B}{V_0 \prod_{j=1}^{i} N_j} + \frac{C}{\left(V_0 \prod_{j=1}^{i} N_j\right)^2} + \frac{D}{\left(V_0 \prod_{j=1}^{i} N_j\right)^3}\right] \tag{21}$$

If the number of experimental pressures, p_i, exceeds the number of adjustable parameters (i.e., B, C, D, V_0), Equation 21 represents an overdetermined system and requires a nonlinear least squares optimization (see Waxman and Hastings 1971) to obtain B, C, D, V_0.

Thus, by means of the Burnett method, one can obtain the molar volume of the sample without having to measure it directly. The accuracy of volumes determined in this way is better than 0.1%. The tradeoffs are the need for highly accurate pressure measurements requiring the use of a dead-weight gauge and a complex data analysis procedure. In this work, a series of Burnett expansions were carried out at a single reference temperature for each fluid (368.15 K [203.00°F] for R134a; 433.15 K [320.00°F] for R123). This allowed a determination of the virial coefficients at the reference temperature.

The bulk of the measurements were taken in the isochoric mode of operation. In this mode, sample is loaded into the volume V_1 only and the pressure is measured over a range of temperatures at a constant density (or volume). This mode of operation has been automated (Linsky et al. 1987), making use of the digital quartz Bourdon pressure

gauge. The molar volume is determined from the pressure measured at the reference isotherm and Equation 20; a previously determined correction for the effect of pressure and temperature on cell volume has also been applied. Once measurement along an isochore is completed, the sample is returned to the reference temperature, expanded into volume V_2, and the process repeated. Measurements were made for a common set of temperatures for each isochore. Thus virial coefficients at these other temperatures could be determined by fitting the data with Equation 20.

A dew point temperature was also obtained for each of the isochores by cooling the sample into the two-phase region. A plot of pressure vs. temperature displays a sharp change of slope at the dew point. The intersection of simple functions fit to the single- and two-phase data gives an accurate determination of the temperature and pressure corresponding to a given (saturated vapor) volume.

Five isochores were measured for each of the fluids in question, resulting in a total of 56 p-V-T points for R134a and 64 points for R123. The minimum volume (maximum density) was approximately twice the critical volume; temperatures ranged from saturation to a maximum of 423 K (302°F) for R134a and 453 K (356°F) for R123.

Liquid Density

Saturated liquid densities were measured in a variable-volume cell originally designed for critical point determinations (Davis 1983; Morrison and Kincaid 1984). The cell consists of a drawn sapphire tube having a volume of approximately 7.0 cm^3 (0.43 in^3); the tube is closed off at each end with stainless steel plugs sealed with O-rings. The sample volume was changed by raising or lowering a column of mercury introduced through an opening in the bottom plug. The total volume accessible to the sample and the volumes of the individual phases within the cell were determined by measuring with a cathetometer the position of the liquid-vapor and liquid-mercury meniscis relative to the top and bottom of the cell. The cell was immersed in a water or ethylene glycol-water bath whose temperature was measured with a platinum resistance thermometer calibrated to 1 mK (0.002°F).

Samples were distilled from a gas buret at room temperature into an intermediate stainless steel cell at liquid nitrogen temperature. The mass of sample transferred was determined in two ways: first, by direct weighing of the cell before and after filling and, second, by using temperature-pressure-volume measurements from the gas buret in conjunction with the virial equation of state. The two determinations typically agreed with one another to 0.1%. The sample was transferred from the stainless steel cell into the sapphire cell by displacement with mercury. The amount of sample was selected to fill the cell roughly one-half full of liquid. At a given temperature, a series of measurements was made with increasing heights of mercury (i.e., with decreasing volumes occupied by the vapor). The volume for the entire sample charge to be at saturated liquid conditions was obtained by extrapolation to zero vapor volume.

The variable-volume apparatus was used to measure the saturated liquid density of R134a from 268 K (23°F) to the critical temperature and R123 from 303 K (86°F) to 373 K (212°F). The accuracy of these densities is ±0.5%. A problem encountered in these measurements was leakage through the O-ring seals. Since the determination of density depends on knowing the amount of sample in the cell, any leakage will result in a decrease in accuracy. R123 presented a particular problem with leakage. While no completely satisfactory material was found, a viton O-ring did contain the R123 sample for several days. This permitted the measurements to proceed, although necessitating frequent changes of sample and replacement of the O-rings. This apparatus was also used to measure vapor pressure and critical point parameters, as described below.

For R123, the liquid density was determined in two additional ways. At temperatures below the normal boiling point, the density was determined by a simple buoyancy technique. A fused silica sphere of known density was suspended from an analytical balance and weighed both in air and immersed in the fluid. At higher temperatures, the constant-volume cell (described below in the section on critical point determination) was also used.

Vapor Pressure

The vapor pressures of R134a and R123 were measured in three different ways on two apparatus. These different methods allow a wider range of temperature to be covered and also serve as a consistency check.

The saturation pressure corresponding to each of the isochores measured on the Burnett p-V-T apparatus was determined by cooling slightly into the two-phase region as described above for the determination of saturated vapor volume. In the second method on this apparatus, the sample chamber was filled approximately one-half full of liquid. The temperature of the oil bath was changed in steps of 5 K (9°F) and the pressure was measured after temperature equilibrium had been reached. Vapor pressures from 313-373 K (104°-212°F) for R134a and from 338-453 K (149°-356°F) for R123 were measured with an accuracy of 0.2 kPa (0.03 psia). There was excellent agreement between the pressures measured with only a small amount of liquid present and those with the sample chamber half full of liquid.

The variable-volume apparatus was also used for vapor pressure measurements. A diaphragm-type pressure transducer was connected to the sapphire sample cell via a mercury-filled capillary coming off the bottom of the cell. Pressures were measured simultaneously and at the same temperatures as the volume measurements. For pure fluids, the pressure should not change with the volume accessible to the sample as long as two phases are present; such a lack of volume dependence on pressure was, in fact, observed to the accuracy level of the pressure transducer. This apparatus was used to measure R134a vapor pressures from 268 K (23°F) to the critical temperature and R123 values from 303 K (86°F) to 373 K (212°F) at an accuracy of 1%.

Critical Point

The critical point of R134a was measured in the variable-volume apparatus described above. At the critical density, the volumes of the liquid and vapor phases formed as the sample is cooled from above the critical point will be identical; that is, the meniscus will appear at the middle of

the cell. In principle, the critical point could be determined by either raising or lowering the temperature. The presence of even minor impurities, which inevitably segregate into one phase or the other in the two-phase region, can cause a specious critical point determination if based on the disappearance of the meniscus upon heating the sample. The formation of the two phases from a carefully prepared homogeneous fluid leads to a more accurate critical point determination.

The sample was heated above the critical temperature, vigorously stirred, and then slowly cooled (approximately 0.05 K/h, 0.09°F/h). The approach to the critical point is accompanied by the strong scattering of the blue part of the visible spectrum, giving the sample a characteristic reddish-brown color when viewed by transmitted light and a pearly blue color by scattered light. The formation of two phases is marked by a sudden loss of the color. After phase separation, the sample was allowed to stand and settle at a constant temperature; the location of the meniscus was then measured. This procedure was repeated at least three times with the volumes varied by about 1% so that the meniscus appeared above, near, and below the center of the cell. These measurements were interpolated to find the conditions at which the meniscus would have appeared exactly in the center (i.e., the critical point).

By these measurements, the critical parameters of R134a were determined as

T_c = 374.205 ± 0.010 K (213.900 ± 0.018°F)
ρ_c = 4056 ± 10 kPa (588.3 ± 1.5 psia)
ρ_c = 515.3 ± 1 kg/m³ (32.2 ± 0.1 lb/ft³)

These values are in good agreement with other measured values. Kabata et al. (1988) report

T_c = 374.30 ± 0.01 K (214.07 ± 0.02°F)
ρ_c = 508 ± 3 kg/m³ (31.7 ± 0.2 lb/ft³).

The slightly higher critical temperature reported by Kabata et al. would be consistent with their technique of observing the disappearance of the liquid-vapor meniscus. The critical temperature measured by Wilson and Basu (1988) is

T_c = 374.25 ± 0.15 K (213.98 ± 0.27°F)

Wilson and Basu did not directly measure the critical pressure and density, but their values determined by extrapolation are also in good agreement with the values presented here.

The critical point for R123 was measured using a constant-volume cell consisting of two sapphire disks approximately 25 mm (1.0 in) in diameter with a spacing of 12.7 mm (0.50 in) supported within a stainless steel housing (Hocken et al. 1975). The cell was sealed with gold foil compression seals, avoiding the problems associated with elastomeric O-rings. The cell was loaded to slightly above the critical density and immersed in a silicon oil bath with the temperature controlled to 0.01 K (0.02°F). The sample was heated until there was a single phase, stirred vigorously, and then cooled until a meniscus appeared. On successive runs, small amounts of the sample were bled from the cell until, as discussed above; a set of measurements spanning the critical point had been made. The cell with its contents was weighed after each run, thus allowing the density at the point of phase separation to be evaluated. The critical parameters determined in this way were

T_c = 456.94 ± 0.03 K (362.82 ± 0.05°F)
ρ_c = 550 ± 5 kg/m³ (34.3 ± 0.3 lb/ft³)

The critical pressure was not directly measured but was determined by extrapolation of the vapor pressure data to the critical temperature; the value thus obtained was

p_c = 3676 ± 10 kPa (533.2 ± 1.5 psia)

There are, to our knowledge, no other documented determinations of the critical parameters of R123 with which to compare these values.

Speed of Sound

The heat capacity of the ideal gas state, as well as virial coefficients, were evaluated from speed of sound data. In the limit of zero frequency, the speed of sound, u, is a thermodynamic quantity which is related to other quantities by the expression

$$u^2(p, T) = \frac{k^0(T)}{M}(RT + \beta_a(T)\,p + \gamma_a(T)\,p^2 + \ldots) \quad (22)$$

where

$$k^0 \equiv C_p^0/C_v^0 = \frac{1}{1-R/C_p^0} \quad (23)$$

R is the gas constant, M is the relative molecular mass, and β_a and γ_a are the acoustic virial coefficients. The second acoustic virial coefficient, β_a, is related to the "ordinary" second virial coefficient, B (such as that determined by the Burnett measurements described above), by

$$\beta_a(T) = 2B + 2(k^0-1)\,T\frac{dB}{dT} + \frac{(k^0-1)^2}{k^0}\,T^2\frac{d^2B}{dT^2} \quad (24)$$

By measuring the speed of sound along an isotherm over a range of pressures, C_p^0, β_a, γ_a, etc., can be evaluated at that temperature by a least squares optimization. The evaluation of B *from* β_a involves temperature derivatives of B. Thus it is convenient to assume a functional form for the temperature dependence of B; the form used here is that derived for hypothetical molecules interacting via the square well potential (Ewing et al. 1988):

$$B(T) = e_1 + e_2 \exp(e_3/T) \quad (25)$$

This functional form allows the evaluation of the derivatives in Equation 24 and, hence, the evaluation of the coefficients e_1, e_2, and e_3 in Equation 25 by a nonlinear least squares optimization.

The method used here for measuring the speed of sound was first proposed by Moldover et al. (1979) and first demonstrated by Mehl and Moldover (1981). The gas of interest is contained within a thick-walled spherical cavity, which itself is contained within an isothermal enclosure. The resonant frequencies of the radially symmetric oscillations of the gas are measured by means of a sonic transmitter and a detector mounted flush with the inside of the cavity. The speed of sound is related to these frequencies, $f_{0,n}$ by

$$u = f_{0,n}\,V_r^{1/3}/\nu_{0,n} \quad (26)$$

where V_r is the volume of the spherical cavity and $\nu_{0,n}$ are

eigenvalues that are known exactly. In practice, V_s is determined from sound speed measurements with argon, a gas for which the speed of sound is very accurately known. Several small (< 0.016%) corrections were made to the measured frequencies to account for heat conduction from the gas into and out of the shell during the course of each acoustic cycle and to account for the elastic response of the spherical shell.

Measurements were made on 13 isotherms for R134a spanning the temperature range 233.15 to 340 K (−40.0° to 152.3°F); for R123, six isotherms over the temperature range 260 to 335 K (8.3° to 143.3°F) were measured. The pressure was varied from 5% to 50% of the saturation pressure at each of the temperatures. The instrumental errors in the measurements of the frequencies, temperatures, and pressures were insignificant. Small (0.01%) inconsistencies in the sound speed data for the refrigerants were observed. These probably resulted from the slow dissolution of the sample into several fluoro-elastomer components of the apparatus. The resulting accuracy for the heat capacities is ±0.1%. Although not presented in detail here, the second virial coefficients derived from the sound speed measurements using Equations 24 and 25 were in excellent agreement with those measured in the Burnett apparatus.

Surface Tension

Surface tension is a fluid property required in many two-phase heat transfer correlations. Surface tension influences the growth of bubbles in nucleate boiling and the drainage of condensate from certain enhanced condenser surfaces. The surface tensions of R134a and R123 were measured using a differential capillary rise technique similar to that described by Rathjen and Straub (1973) in combination with density data. The temperature range was 263 to 368 K (14° to 203°F) for R134a and 248 to 413 K (−13° to 284°F) for R123. The capillary height, h_i, was measured in at least two different capillaries to a resolution of ±0.02 mm (±0.0008 in) with a cathetometer. The difficult measurement of the bulk meniscus height, h_o, was avoided by the two-capillary method. The experimental measurements determined the capillary length parameter, α^2, through the relation derived by Rayleigh (1916):

$$\alpha^2 = r_i \left[h_i - h_o + \frac{r_i}{3} - 0.1288 \frac{r_i^2}{(h_i - h_o)} + 0.1312 \frac{r_i^3}{(h_i - h_o)^2} \right] \quad (27)$$

where r_i is the capillary radius. In this work four different capillaries, with radii ranging from 0.148 to 0.574 mm (0.0058 to 0.0226 in), were used in order to increase the dynamic range of the measurements. The surface tension is related to α^2 through

$$\sigma = \alpha^2 \Delta \rho g / 2 \quad (28)$$

where $\Delta\rho$ is the difference between the liquid and vapor densities and g is the acceleration due to gravity. Density values calculated from the equation of state were used to compute surface tension values. The parameter α^2 is represented by the form (Chaar et al. 1986):

$$\alpha^2 = \alpha_0^2 \tau^{0.934} \quad (29)$$

where $\tau = 1 - T/T_c$; $\alpha_0^2 = 6.35$ mm² for R134a and 5.75 mm² for R123. Experimental and calculated values of surface tension are shown in Figure 1. The estimated accuracy of the values is ±0.0001 N/m (±0.1 dyn/cm). The surface tensions were also correlated directly as

$$\sigma = \sigma_0 \tau^{1.26} \quad (30)$$

where $\sigma_0 = 0.0608$ N/m (60.8 dyn/cm) for R134a and $\sigma_0 = 0.0575$ N/m (57.5 dyn/cm) for R123. Although more convenient than Equations 28 and 29, Equation 30 is not as accurate, leading to errors of as much as 0.00025 N/m (0.25 dyn/cm).

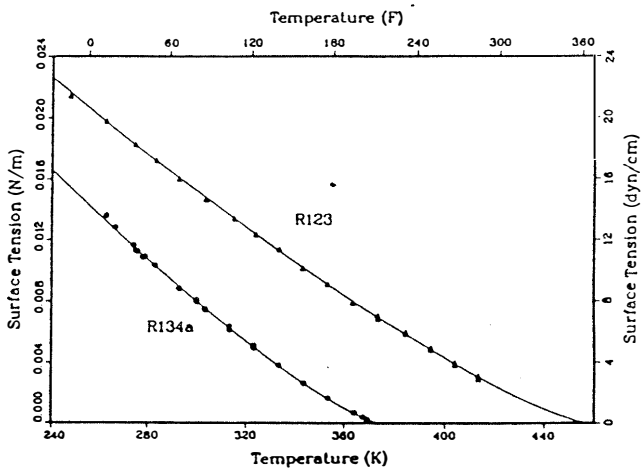

Figure 1 *Surface tension as a function of temperature for R134a and R123; symbols are experimental points, lines are correlation.*

Fluid Samples

The sample of R134a was stated by the manufacturer to have a purity of approximately 99.94 wt%. The major impurities were related fluorocarbons, which should have an insignificant effect on the measured properties at the levels present, and water. The sample of R123 was assayed by the manufacturer as 99.99 wt% pure with a water content of less than 20 parts per million (ppm). An analysis conducted in this laboratory using gas chromatography and mass spectroscopy techniques confirmed this result. A trace quantity of the isomer R123a (1,2-dichloro-1,2,2-trifluoroethane) was detected. The amount of R123a was barely above noise levels and thus could not be quantified, but should be no more than a few parts per million.

Both samples were found to contain significant quantities of air. (The purity values stated above are on an air-free basis.) The air, along with any other highly volatile impurities, was removed by repeatedly freezing the sample at liquid nitrogen temperatures, evacuating, and thawing.

The sound speed measurements are sensitive to any water present as an impurity and thus significant effort was devoted to analyzing for water content. The R134a was analyzed by gas chromatography using a 2 m packed column and a thermal conductivity detector. Calibration was done using four gravimetrically prepared standards of water in nitrogen. The water content of the R134a as received was 215 ± 8 ppm. The sample used in the sound

speed measurements was dried by passing over a molecular sieve to a level of 105 ± 5 ppm water. A similar technique was used for R123 except that the sample was injected as a liquid into the GC column using a cooled syringe, and gravimetrically prepared acetonitrile/water calibration standards were used. This analysis yielded a R123 water content of 23 ± 2 ppm as received and 8 ± 2 ppm for the dried sample used in the sound speed measurements. An analysis of R123 by a second method, a Karl Fischer titration, yielded a water content of between 12 and 35 ppm.

The water content of the dried samples was sufficiently low to not affect the sound speed measurements. There was no detectable difference in critical point between dried and undried samples of R134a.

FORMULATION OF THERMODYNAMIC SURFACE

The previous discussion outlined how an equation of state could encompass all of the thermodynamic properties of a fluid. Not all equations of state, however, are applicable to the entire thermodynamic surface. For example, the Martin-Hou equation, which is often applied to refrigerants (ASHRAE 1986), is not accurate in the liquid region. With this and many other equations of state, separate correlations for saturated liquid density and vapor pressure are required. A single equation, applicable to both the liquid and vapor phases, from which all the thermodynamic properties can be computed in a thermodynamically consistent way, is desired; two such equations were investigated for use with R134a and R123.

CSD Equation of State

The Carnahan-Starling-DeSantis (CSD) equation of state has been applied to refrigerants and, particularly, refrigerant mixtures (Morrison and McLinden 1985, 1986). It is of the form

$$\frac{pV}{RT} = \frac{1+y+y^2-y^3}{(1+y)^3} - \frac{a}{RT(V+b)} \qquad (31)$$

where $y = b/4V$. The first term on the right side of Equation 31 is the Carnahan-Starling (1969) representation of the behavior of a system of rigid, noninteracting spherical molecules; the parameter "b" is related to this "hard-sphere" volume. The second term, proposed by DeSantis et al. (1976), accounts for the long-range attractive forces between molecules; the parameter "a" characterizes this interaction. The parameters "a" and "b" are temperature-dependent and are represented as:

$$a = a_0 \exp(a_1 T + a_2 T^2) \qquad (32)$$

$$b = b_0 + b_1 T + b_2 T^2 \qquad (33)$$

The attributes of a strong theoretical basis and relative simplicity allow the CSD equation to represent a fluid with a minimum of data. The CSD equation was fitted to the present experimental data. The accuracy with which the CSD equation represented the properties of R123 was good; however, the fit to the R134a data, while usable, was not of a level commensurate with the accuracy of the experimental data. This failure may be due to the highly polar nature of these new fluids and necessitated fitting a more complex equation of state. Given the high accuracy data now available for these fluids, it is appropriate to employ a more sophisticated equation of state. For consistency, the MBWR equation of state will be used for both R134a and R123.

Modified BWR Equation of State

A modification of the Benedict-Webb-Rubin equation of state (MBWR) proposed by Jacobsen and Stewart (1973) is adopted here. It is versatile, applicable over wide ranges of temperature and pressure, and has found wide acceptance for the representation of hydrocarbons and cryogenic fluids (e.g., Younglove 1982; Younglove and Ely 1987); it has also seen limited application to the halocarbon refrigerants (ASHRAE 1986). It is of the form

$$p = \sum_{n=1}^{9} a_n / V^n + \exp(-V_c^2/V^2) \sum_{n=10}^{15} a_n / V^{2n-17} \qquad (34)$$

where the temperature dependence of the coefficients is given by

$$\begin{aligned}
a_1 &= RT \\
a_2 &= b_1 T + b_2 T^{0.5} + b_3 + b_4/T + b_5/T^2 \\
a_3 &= b_6 T + b_7 + b_8/T + b_9/T^2 \\
a_4 &= b_{10} T + b_{11} + b_{12}/T \\
a_5 &= b_{13} \\
a_6 &= b_{14}/T + b_{15}/T^2 \\
a_7 &= b_{16}/T \\
a_8 &= b_{17}/T + b_{18}/T^2 \\
a_9 &= b_{19}/T^2 \\
a_{10} &= b_{20}/T^2 + b_{21}/T^3 \\
a_{11} &= b_{22}/T^2 + b_{23}/T^4 \\
a_{12} &= b_{24}/T^2 + b_{25}/T^3 \\
a_{13} &= b_{26}/T^2 + b_{27}/T^4 \\
a_{14} &= b_{28}/T^2 + b_{29}/T^3 \\
a_{15} &= b_{30}/T^2 + b_{31}/T^3 + b_{32}/T^4
\end{aligned} \qquad (35)$$

The greater complexity of the MBWR equation of state compared to the CSD equation, along with the flexibility allowed by its 32 adjustable parameters, allows a much more accurate representation of the experimental data but simultaneously entails a more involved fitting procedure.

Auxiliary Functions

In order to fit the saturation boundary (which is given heavy weight) in a straightforward way, information on the saturated liquid and vapor densities and vapor pressure as well as their temperature derivatives, all at common temperatures, is required. Since such data are seldom available, the saturation data are first fit to separate functions, which are then used to compute the required points. These auxiliary functions are used only in the fitting pro-

cess; the final computation of all thermodynamic quantities is based directly on the MBWR equation of state.

The measured vapor pressure values were fit to the form

$$\ln p = \pi_1/T + \pi_2 + \pi_3 T + \pi_4(1 - T/T_c)^{1.5} \quad (36)$$

The coefficients, π_i, are given in Table 1. (Critical region theory predicts a value of 1.9 for the exponent in the last term of Equation 36; a value of 1.5, however, was empirically found to yield a better fit over a wide temperature range.) For R134a, there are data from three apparatus and two independent sources. For the temperature range where they overlap (above 310.0 K or 98.3°F), the data of Wilson and Basu and those measured here on the Burnett apparatus are in excellent agreement with RMS deviations from Equation 36 of 0.11% and 0.07%, respectively. At lower temperatures, the data from the variable-volume apparatus are consistently lower than those of Wilson and Basu. The difference is greatest (approximately 3%) at 268 K (23°F). In fitting Equation 36, a higher weight was given to the data from the Burnett apparatus, reflecting their higher accuracy compared to the variable-volume apparatus. The data of Wilson and Basu were also included because of their high stated accuracy and greater temperature range (down to 211.0 K or −79.9°F). The overall weighted RMS deviation for R134a was 0.20%. For R123, the RMS deviations from the fit were 0.07 and 0.39% for the Burnett and variable-volume apparatuses, respectively, with an overall weighted RMS deviation of 0.15%. Again, the data from the Burnett apparatus were given a higher weight.

TABLE 1
Coefficients for the Auxiliary Functions and C_p^o

	R134a	R123
Constants for use with Equations 22, 36–40:		
SI Units		
T_c (K)	374.205	456.94
ρ_c (kg/m^3)	515.3	549.9
B	0.34	0.333
M	102.030	152.930
I-P Units		
T_c (°R)	673.57	822.49
ρ_c (lb/ft^3)	32.17	34.33
β	0.34	0.333
M	102.030	152.930
Vapor pressure, Equation 36		
SI Units (p in kPa; T in K)		
π_1	−3.353 46 E + 3	−3.991 71 E + 3
π_2	1.836 06 E + 1	1.803 35 E + 1
π_3	−2.908 04 E − 3	−2.377 67 E − 3
π_4	2.783 66 E + 0	2.812 72 E + 0
I-P Units (p in psia; T in °R)		
π_1	−6.036 23 E + 3	−7.185 08 E + 3
π_2	1.642 99 E + 1	1.610 28 E + 1
π_3	−1.615 58 E − 3	−1.320 93 E − 3
π_4	2.783 66 E + 0	2.812 72 E + 0
Saturated liquid density, Equation 37 (dimensionless)		
d_1	1.723 89	1.882 64
d_2	1.717 61	0.257 94
d_3	−2.269 04	0.680 74
d_4	1.707 44	−0.101 91
Saturated vapor density, Equation 40 (dimensionless)		
g_1	−3.479 66	−4.915 71
g_2	9.349 04	18.877 51
g_3	−0.401 86	−17.601 47
g_4	28.090 01	41.639 63
g_5	31.910 04	33.899 77
Ideal gas heat capacity, Equation 41		
SI Units (C_p^0 in J/(mol · K); T in K)		
c_1	1.940 06 E + 1	2.926 04 E + 1
c_2	2.585 31 E − 1	3.029 94 E − 1
c_3	−1.296 65 E − 4	−1.929 07 E − 4
I-P Units (C_p^0 in BTU/(lb mol · °R)		
c_1	4.636 94 E + 0	6.993 53 E + 0
c_2	3.432 86 E − 2	4.023 26 E − 2
c_3	−9.565 19 E − 6	−1.423 05 E − 5

The saturated liquid densities were fit to the form:

$$\rho/\rho_c = 1 + d_1 \tau^{\beta} + d_2 \tau^{2/3} + d_3 \tau + d_4 \tau^{4/3} \quad (37)$$

where $\tau = (1 - T/T_c)$ and ρ_c is the critical density. The coefficients for the fit to R134a and R123 are given in Table 1. The value of the critical exponent, β, is taken as 0.34 for R134a based on the work of Kabata et al. (1988); it is assumed to be 1/3 for R123. A comparison of experimental values with those calculated by Equation 37 is given in Figure 2 for 134a. There are significant differences, as large as 1.5%, especially near the critical temperature, between the different sources. At this time, there is little justification for selecting one source over another and thus all were given equal weight in the fit. The RMS deviations between the experimental values and the auxiliary function are 0.44% for the variable-volume apparatus, 0.38% for the data of Wilson and Basu, and 0.24% for the data of Kabata et al. A similar comparison for R123 is given in Figure 3. For this fluid, all of the data are from this work but by three different methods, as described above. There is good agreement between the various techniques with RMS deviations from Equation 37 of 0.06% for the low-temperature buoyancy technique, 0.34% for the variable-volume apparatus, and 0.16% for the constant-volume apparatus.

The fitting of an auxiliary function for saturated vapor density presents a special problem; the experimental values from the Burnett apparatus extend over a limited temperature range (320 to 366 K or 117° to 199°F for R134a and 340 to 425 K or 152° to 305°F for R123). Densities at lower temperatures were generated by the truncated virial equation of state:

$$V = RT/p + B \quad (38)$$

$$\rho = M/V \quad (39)$$

where M is relative molecular mass; the pressure, p, is computed at saturation conditions by Equation 36; and the second virial coefficient, B, is based on sound speed data and is given by Equation 25. These calculated points were combined with values from the Burnett apparatus and fitted to the following form:

$$\ln(\rho/\rho_c) = g_1 \tau^{\beta} + g_2 \tau^{2/3} + g_3 \tau + g_4 \tau^{4/3} + g_5 \ln(T/T_c) \quad (40)$$

Again the coefficients are given in Table 1. The virial equation of state truncated at the second virial coefficient is accurate only for low to moderate pressures; this translated into an upper temperature limit of 273 K (32°F) for R134a and 323 K (122°F) for R123. There is thus a significant temperature span where no information on saturated

vapor volumes is available. Equation 36 should, however, adequately interpolate between the high-temperature Burnett measurements and the lower temperature calculated values. The RMS deviations were 0.09% for both R134a and R123.

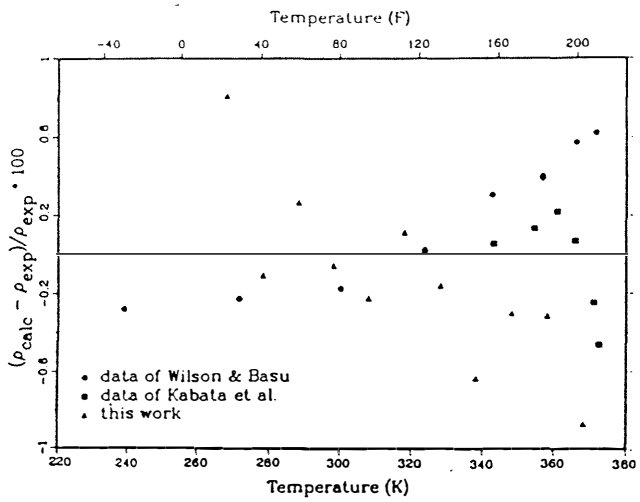

Figure 2 Comparison of experimental saturated liquid densities with correlation, R134a

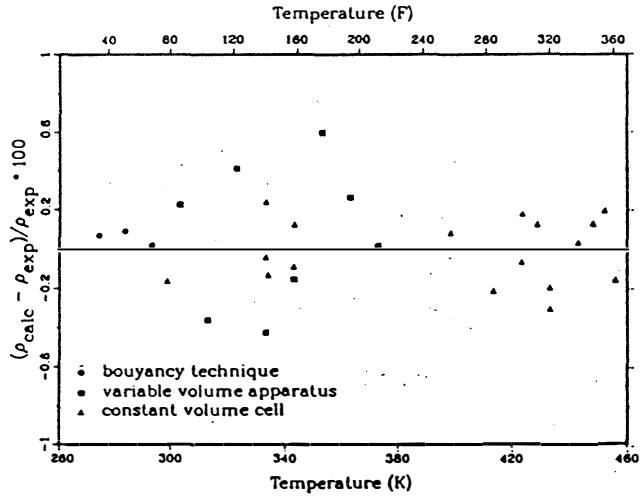

Figure 3 Comparison of experimental saturated liquid densities with correlation, R123

P-V-T Surface

The isochoric p-V-T measurements made with the Burnett apparatus along with the second virial coefficients derived from the sound speed and Burnett measurements were used, along with the auxiliary functions for the saturation boundary, to fit the MBWR equation of state. For R134a the isochoric measurements of Wilson and Basu were also included.

One advantage of the MBWR equation of state is its ability to represent the entire thermodynamic surface, including the compressed liquid region. There are, however, no experimental compressed liquid data available at the present time with which to fit this region. To resolve this situation, p-V-T values along several isotherms in the compressed liquid region, extending from near saturation to a pressure of approximately 10,000 kPa (1500 psia), were calculated using a property estimation program based on the theory of extended corresponding states (Ely 1984). This method starts with a very accurate thermodynamic surface for a well-characterized reference fluid (in this case, propane), scales this surface by the use of reduced properties (i.e., a property such as temperature divided by that property at the critical point), and then fits a number of "shape factors" to slightly distort the reference surface to reproduce the available experimental vapor pressure and saturated liquid density for the fluid in question. The "data" generated using the extended corresponding states model were given a very low statistical weight compared to the experimental values in fitting the coefficients of the MBWR equation.

The routines developed by Ely (1984) were used with minor modification to fit the MBWR equation of state to the experimental data. These fitting routines employ a multiproperty linear least-squares analysis and incorporate a weighting scheme proposed by McCarty (1980). The resulting coefficients are given in Table 2. The MBWR equation of state is constrained to pass through the critical point.

TABLE 2
Coefficients for the MBWR Equation of State

	R134a	R123
b_1	5.432 351 078 E+01	-3.565 346 146 E+02
b_2	-2.817 179 422 E+03	2.460 182 902 E+04
b_3	4.180 438 062 E+04	-4.886 306 960 E+05
b_4	-3.256 922 234 E+06	6.975 297 669 E+07
b_5	3.083 105 280 E+07	-5.898 504 668 E+09
b_6	-2.306 068 261 E-01	2.020 863 609 E+01
b_7	-1.802 987 614 E+03	-4.091 285 105 E+04
b_8	1.895 347 500 E+06	2.267 025 665 E+07
b_9	1.266 051 930 E+09	3.494 004 970 E+09
b_{10}	1.741 323 933 E-01	-3.856 016 874 E+00
b_{11}	-4.772 988 829 E+01	7.137 009 696 E+03
b_{12}	-3.432 544 166 E+04	-2.373 613 586 E+06
b_{13}	1.686 496 803 E+01	-2.291 124 604 E+01
b_{14}	-6.286 672 309 E+03	-7.786 150 982 E+04
b_{15}	-7.041 712 468 E+05	3.187 411 790 E+06
b_{16}	5.735 386 537 E+02	8.700 369 537 E+03
b_{17}	-1.356 666 658 E+01	-2.108 108 891 E+02
b_{18}	3.072 670 709 E+03	-8.707 384 556 E+04
b_{19}	-8.493 229 270 E+01	4.686 693 868 E+03
b_{20}	-1.849 376 298 E+09	-7.380 524 773 E+09
b_{21}	5.825 639 389 E+10	5.193 095 367 E+10
b_{22}	-6.512 433 009 E+07	-6.105 495 540 E+08
b_{23}	6.341 579 266 E+11	1.634 552 631 E+13
b_{24}	-6.885 139 519 E+05	-1.513 595 925 E+07
b_{25}	-3.691 540 607 E+07	9.576 741 434 E+08
b_{26}	-9.494 108 810 E+03	-3.322 908 616 E+05
b_{27}	-3.083 412 869 E+07	-1.324 816 394 E+10
b_{28}	-1.514 309 042 E+01	-4.461 246 944 E+03
b_{29}	-4.323 050 466 E+03	1.591 820 977 E+06
b_{30}	-2.023 379 823 E-01	-5.971 857 323 E+00
b_{31}	-5.752 269 805 E+01	-3.155 068 205 E+04
b_{32}	-7.535 403 081 E+03	-8.095 134 997 E+05

Note: These coefficients are for pressure in kPa, temperature in K, and volume in L/mol; the gas constant, R = 8.314 471 J/(mol·K).

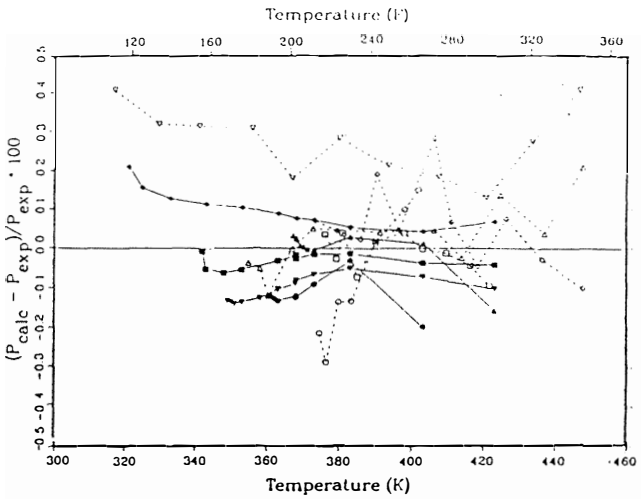

Figure 4 *Comparison of experimental p-V-T data with MBWR equation of state, R134a; solid symbols are data of this work, open symbols are data of Wilson and Basu (1988), lines connect measurements along an isochor.*

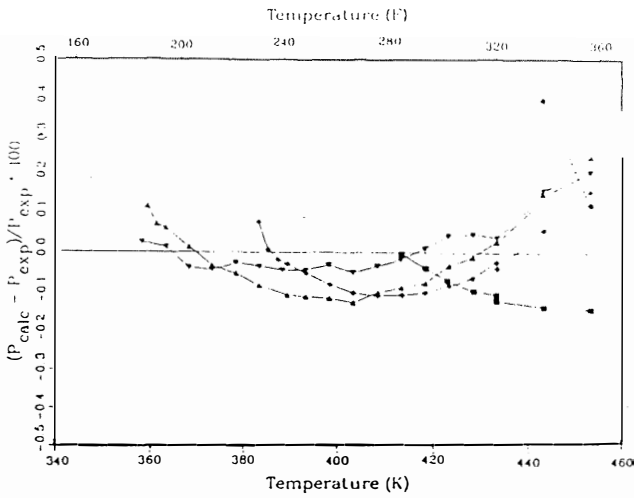

Figure 5 *Comparison of experimental p-V-T data with MBWR equation of state, R123*

The fit of the equation of state in the single-phase region can be assessed by comparing either pressures computed given temperature and volume, or volumes computed given temperature and pressure. A comparison of experimental and calculated pressures is given in Figure 4 for R134a. The isochoric p-V-T values reported by Wilson and Basu and those measured with the Burnett apparatus generally show good agreement. The RMS deviations for the two data sets are very similar (0.09% for the Burnett data vs. 0.15% for Wilson and Basu's data). The lowest density isochore of Wilson and Basu (indicated by open, inverted triangles in Figure 4) appeared to be inconsistent with the other data and was given zero weight in the fit. The RMS deviations for volume are somewhat larger (0.17% for this work, 0.76% for the values of Wilson and Basu). A large share of the total error (especially for the data of Wilson and Basu) is due to a few measurements near the critical point where the pressure-volume isotherms are very "flat," so small differences in pressure or temperature result in large errors in volume.

The average absolute difference between experimental and calculated second virial coefficients was 0.55 cm^3/mol; the maximum difference was 1.04 cm^3/mol corresponding to 0.28%. For temperatures from 233 K (−40°F) to the critical temperature, the MBWR equation of state reproduced the saturated liquid and vapor densities and vapor pressures given by the auxiliary functions with RMS deviations of 0.70%, 0.18%, and 0.03%, respectively. Again, much of the total error is due to the near-critical region; over the more limited temperature range of 233 to 353 K (−40° to 176°F), the RMS errors reduce to 0.03%, 0.10%, and 0.003%. These deviations must be combined with the RMS deviations for the auxiliary functions (presented above) to obtain the differences between the MBWR equation of state and the actual experimental values.

The residuals for the R123 p-V-T data are presented in Figure 5. A small (approximately 0.1%) systematic deviation with temperature is observed. The RMS deviation for the 64 p-V-T points is 0.10% in pressure and 0.15% in volume. The average absolute deviation in the experimental and calculated second virial coefficients is 1.32 cm^3/mol. Along the saturation boundary, the MBWR reproduces the liquid density with an RMS error of 0.71%, the vapor density to 0.29%, and the vapor pressure to 0.03%. As with R134a, most of the total RMS error is due to the near-critical region. Over the temperature range of 279.9 to 430.0 K (26.3 to 314.3°F), the RMS errors reduce to 0.07% for liquid density, 0.12% for vapor density, and 0.010% for vapor pressure, respectively.

Because of the necessity to estimate compressed liquid p-V-T values, the accuracy of the MBWR equation of state in this region cannot be stated. However, because its behavior in this region is based on a real reference fluid (rather than being an extrapolation of vapor and saturated liquid behavior), the modest amounts of subcooling usually encountered in refrigeration systems should be represented with good accuracy.

Ideal Gas Heat Capacity

The ideal gas heat capacities derived from the sound speed measurements were fitted to a simple polynomial in temperature:

$$C_p^o = c_1 + c_2 T + c_3 T^2 \qquad (41)$$

where the coefficients are given in Table 1. The RMS deviations between Equation 41 and the experimental values were 0.04% for R134a and 0.17% for R123 over the temperature range of the data. The values for R134a measured here are 1.2% to 1.7% lower than those reported by Chen et al. (1975) and 1.4% to 2.7% lower than the values reported by Wilson and Basu with the greater differences at the higher temperatures. For R123, the value measured here at 305 K (89°F) is 0.6% higher than the value reported by Luft (1954). The values of Chen et al., Wilson and Basu, and Luft are calculated using statistical mechanics and the assignment of molecular vibrational modes based on spectroscopic data. Although this method of calculating C_p^o is, in principle, highly accurate, the assignment of the various spectral lines to specific vibrational modes of the

Table 3a
Saturation Properties for R134a; SI Units

Temp (°C)	Pressure (kPa)	Density (kg/m³)		Enthalpy (kJ/kg)		Entropy (kJ/kg·K)		C_v (kJ/kg·K)		C_p (kJ/kg·K)		σ (N/m)	Temp (°C)
		liq	vap	liq	vap	liq	vap	liq	vap	liq	vap		
-40.	52.	1414.	2.8	0.0	223.3	0.000	0.958	0.667	0.646	1.129	0.742	0.0177	-40.
-35.	66.	1399.	3.5	5.7	226.4	0.024	0.951	0.696	0.659	1.154	0.758	0.0169	-35.
-30.	85.	1385.	4.4	11.5	229.6	0.048	0.945	0.722	0.672	1.178	0.774	0.0161	-30.
-25.	107.	1370.	5.5	17.5	232.7	0.073	0.940	0.746	0.685	1.202	0.791	0.0154	-25.
-20.	133.	1355.	6.8	23.6	235.8	0.097	0.935	0.767	0.698	1.227	0.809	0.0146	-20.
-15.	164.	1340.	8.3	29.8	238.8	0.121	0.931	0.786	0.712	1.250	0.828	0.0139	-15.
-10.	201.	1324.	10.0	36.1	241.8	0.145	0.927	0.803	0.726	1.274	0.847	0.0132	-10.
-5.	243.	1308.	12.1	42.5	244.8	0.169	0.924	0.817	0.740	1.297	0.868	0.0124	-5.
0.	293.	1292.	14.4	49.1	247.8	0.193	0.921	0.830	0.755	1.320	0.889	0.0117	0.
5.	350.	1276.	17.1	55.8	250.7	0.217	0.918	0.840	0.770	1.343	0.912	0.0110	5.
10.	415.	1259.	20.2	62.6	253.5	0.241	0.916	0.849	0.785	1.365	0.936	0.0103	10.
15.	489.	1242.	23.7	69.4	256.3	0.265	0.914	0.857	0.800	1.388	0.962	0.0096	15.
20.	572.	1224.	27.8	76.5	259.0	0.289	0.912	0.863	0.815	1.411	0.990	0.0089	20.
25.	666.	1206.	32.3	83.6	261.6	0.313	0.910	0.868	0.831	1.435	1.020	0.0083	25.
30.	771.	1187.	37.5	90.8	264.2	0.337	0.908	0.872	0.847	1.460	1.053	0.0076	30.
35.	887.	1167.	43.3	98.2	266.6	0.360	0.907	0.875	0.863	1.486	1.089	0.0069	35.
40.	1017.	1147.	50.0	105.7	268.8	0.384	0.905	0.878	0.879	1.514	1.130	0.0063	40.
45.	1160.	1126.	57.5	113.3	271.0	0.408	0.904	0.881	0.896	1.546	1.177	0.0056	45.
50.	1318.	1103.	66.1	121.0	272.9	0.432	0.902	0.883	0.914	1.581	1.231	0.0050	50.
55.	1491.	1080.	75.9	129.0	274.7	0.456	0.900	0.886	0.932	1.621	1.295	0.0044	55.
60.	1681.	1055.	87.2	137.1	276.1	0.479	0.897	0.890	0.950	1.667	1.374	0.0038	60.
65.	1888.	1028.	100.2	145.3	277.3	0.504	0.894	0.895	0.970	1.724	1.473	0.0032	65.
70.	2115.	999.	115.5	153.9	278.1	0.528	0.890	0.901	0.991	1.794	1.601	0.0027	70.
75.	2361.	967.	133.6	162.6	278.4	0.553	0.885	0.910	1.014	1.884	1.776	0.0022	75.
80.	2630.	932.	155.4	171.8	278.0	0.578	0.879	0.922	1.039	2.011	2.027	0.0016	80.
85.	2923.	893.	182.4	181.3	276.8	0.604	0.870	0.937	1.066	2.204	2.408	0.0012	85.
90.	3242.	847.	216.9	191.6	274.5	0.631	0.860	0.958	1.097	2.554	3.056	0.0007	90.
95.	3590.	790.	264.5	203.1	270.4	0.662	0.844	0.988	1.131	3.424	4.483	0.0003	95.
100.	3971.	689.	353.1	219.3	260.4	0.704	0.814	1.044	1.168	10.793	14.807	0.0000	100.

Table 3b
Saturation Properties for R134a; I-P Units

Temp (°F)	Pressure (psia)	Density (lb/ft³)		Enthalpy (BTU/lb)		Entropy (BTU/lb·°F)		C_v (BTU/lb·°F)		C_p (BTU/lb·°F)		σ (dyn/cm)	Temp (°F)
		liq	vap	liq	vap	liq	vap	liq	vap	liq	vap		
-40.	7.5	88.2	0.17	0.0	96.1	0.000	0.229	0.159	0.154	0.270	0.177	17.7	-40.
-30.	9.9	87.2	0.23	2.7	97.6	0.006	0.227	0.167	0.158	0.276	0.182	16.8	-30.
-20.	12.9	86.2	0.29	5.5	99.1	0.013	0.226	0.174	0.161	0.283	0.186	16.0	-20.
-10.	16.7	85.2	0.37	8.4	100.5	0.019	0.224	0.180	0.165	0.289	0.190	15.1	-10.
0.	21.2	84.2	0.46	11.3	102.0	0.026	0.223	0.186	0.168	0.296	0.195	14.3	0.
10.	26.6	83.1	0.58	14.3	103.5	0.032	0.222	0.190	0.172	0.302	0.200	13.5	10.
20.	33.1	82.0	0.71	17.4	104.9	0.039	0.221	0.194	0.176	0.308	0.206	12.7	20.
30.	40.8	80.9	0.87	20.5	106.3	0.045	0.220	0.198	0.180	0.314	0.211	11.9	30.
40.	49.8	79.7	1.05	23.7	107.7	0.051	0.219	0.201	0.184	0.320	0.217	11.1	40.
50.	60.2	78.6	1.26	26.9	109.1	0.058	0.219	0.203	0.188	0.326	0.224	10.3	50.
60.	72.1	77.4	1.51	30.2	110.4	0.064	0.218	0.205	0.192	0.332	0.231	9.5	60.
70.	85.9	76.2	1.79	33.6	111.7	0.070	0.218	0.207	0.196	0.339	0.238	8.8	70.
80.	101.5	74.9	2.12	37.0	112.9	0.077	0.217	0.208	0.200	0.345	0.246	8.0	80.
90.	119.1	73.6	2.50	40.5	114.1	0.083	0.217	0.209	0.204	0.352	0.255	7.3	90.
100.	138.9	72.2	2.93	44.0	115.2	0.089	0.217	0.210	0.208	0.359	0.266	6.6	100.
110.	161.1	70.7	3.43	47.6	116.3	0.096	0.216	0.210	0.213	0.367	0.277	5.9	110.
120.	185.9	69.2	4.00	51.3	117.2	0.102	0.216	0.211	0.217	0.376	0.291	5.2	120.
130.	213.3	67.6	4.67	55.1	118.1	0.108	0.215	0.212	0.222	0.386	0.308	4.5	130.
140.	243.8	65.8	5.44	59.0	118.8	0.115	0.214	0.213	0.227	0.399	0.328	3.8	140.
150.	277.4	64.0	6.36	62.9	119.3	0.121	0.214	0.214	0.232	0.414	0.355	3.2	150.
160.	314.4	61.9	7.44	67.0	119.7	0.127	0.212	0.216	0.238	0.433	0.391	2.6	160.
170.	355.1	59.7	8.76	71.3	119.7	0.134	0.211	0.218	0.244	0.459	0.442	2.0	170.
180.	399.9	57.2	10.40	75.7	119.4	0.141	0.209	0.222	0.251	0.498	0.520	1.4	180.
190.	449.2	54.2	12.51	80.4	118.6	0.148	0.207	0.227	0.259	0.566	0.650	0.9	190.
200.	503.4	50.6	15.39	85.6	117.0	0.156	0.203	0.233	0.267	0.721	0.918	0.5	200.
210.	563.2	45.0	20.22	92.3	113.6	0.165	0.197	0.245	0.277	1.549	2.129	0.1	210.

Table 4a
Saturation Properties for R123; SI Units

Temp (°C)	Pressure (kPa)	Density (kg/m³)		Enthalpy (kJ/kg)		Entropy (kJ/kg·K)		C_v (kJ/kg·K)		C_p (kJ/kg·K)		σ (N/m)	Temp (°C)
		liq	vap	liq	vap	liq	vap	liq	vap	liq	vap		
-20.	12.	1571.	0.9	17.2	202.2	0.067	0.798	0.665	0.573	0.838	0.633	0.0209	-20.
-15.	16.	1560.	1.1	21.4	205.2	0.083	0.795	0.670	0.581	0.852	0.642	0.0203	-15.
-10.	20.	1549.	1.4	25.7	208.1	0.100	0.793	0.674	0.590	0.866	0.652	0.0197	-10.
-5.	26.	1537.	1.8	30.1	211.1	0.116	0.792	0.678	0.599	0.881	0.661	0.0191	-5.
0.	33.	1525.	2.2	34.5	214.1	0.133	0.790	0.681	0.607	0.896	0.671	0.0184	0.
5.	41.	1514.	2.8	39.0	217.2	0.149	0.790	0.684	0.616	0.912	0.680	0.0178	5.
10.	51.	1501.	3.4	43.6	220.2	0.166	0.789	0.687	0.624	0.928	0.689	0.0172	10.
15.	62.	1489.	4.1	48.3	223.2	0.182	0.789	0.691	0.632	0.945	0.699	0.0166	15.
20.	75.	1477.	4.9	53.1	226.3	0.198	0.789	0.694	0.640	0.962	0.708	0.0160	20.
25.	91.	1464.	5.9	57.9	229.4	0.215	0.790	0.698	0.648	0.979	0.717	0.0154	25.
30.	109.	1452.	6.9	62.9	232.5	0.231	0.790	0.701	0.655	0.995	0.725	0.0148	30.
35.	130.	1439.	8.2	67.9	235.5	0.247	0.791	0.705	0.662	1.012	0.734	0.0142	35.
40.	154.	1425.	9.6	73.0	238.6	0.264	0.793	0.708	0.669	1.028	0.743	0.0136	40.
45.	181.	1412.	11.2	78.2	241.7	0.280	0.794	0.711	0.675	1.043	0.751	0.0131	45.
50.	212.	1399.	13.0	83.5	244.7	0.297	0.796	0.714	0.681	1.058	0.759	0.0125	50.
55.	247.	1385.	15.0	88.8	247.8	0.313	0.797	0.717	0.686	1.072	0.768	0.0119	55.
60.	286.	1371.	17.3	94.2	250.8	0.329	0.799	0.720	0.692	1.085	0.776	0.0113	60.
65.	330.	1356.	19.8	99.7	253.8	0.345	0.801	0.722	0.697	1.097	0.785	0.0108	65.
70.	378.	1342.	22.6	105.2	256.7	0.361	0.803	0.725	0.701	1.108	0.793	0.0102	70.
75.	431.	1327.	25.8	110.8	259.6	0.377	0.805	0.727	0.706	1.119	0.802	0.0097	75.
80.	490.	1312.	29.2	116.4	262.5	0.393	0.807	0.729	0.710	1.128	0.812	0.0091	80.
85.	555.	1296.	33.1	122.1	265.3	0.409	0.809	0.731	0.714	1.137	0.822	0.0086	85.
90.	626.	1280.	37.3	127.8	268.0	0.425	0.811	0.733	0.718	1.145	0.833	0.0080	90.
95.	704.	1264.	42.0	133.5	270.7	0.440	0.813	0.735	0.722	1.152	0.845	0.0075	95.
100.	788.	1247.	47.2	139.3	273.3	0.456	0.815	0.737	0.726	1.160	0.859	0.0070	100.
105.	880.	1230.	52.9	145.1	275.8	0.471	0.817	0.739	0.730	1.167	0.874	0.0065	105.
110.	979.	1212.	59.2	150.9	278.2	0.486	0.818	0.740	0.734	1.174	0.891	0.0060	110.
115.	1087.	1193.	66.1	156.8	280.5	0.501	0.820	0.742	0.738	1.182	0.911	0.0054	115.
120.	1203.	1173.	73.8	162.7	282.7	0.516	0.821	0.744	0.743	1.191	0.933	0.0050	120.
125.	1327.	1153.	82.3	168.6	284.8	0.531	0.822	0.746	0.749	1.202	0.960	0.0045	125.
130.	1461.	1131.	91.8	174.6	286.7	0.545	0.823	0.748	0.755	1.215	0.992	0.0040	130.
135.	1605.	1109.	102.3	180.6	288.5	0.560	0.824	0.750	0.763	1.232	1.030	0.0035	135.
140.	1760.	1085.	114.1	186.7	290.2	0.574	0.825	0.753	0.771	1.253	1.076	0.0031	140.
145.	1925.	1060.	127.3	192.8	291.7	0.589	0.825	0.757	0.781	1.281	1.132	0.0026	145.
150.	2102.	1033.	142.4	199.0	292.9	0.603	0.825	0.763	0.793	1.317	1.202	0.0022	150.

molecule is often ambiguous (as demonstrated by the differing values obtained by Chen et al. and Wilson and Basu). Given the high precision and accuracy of the sound speed measurements, ideal gas heat capacities based solely on those data are adopted here (except that Luft's data for R123 at 400 K [260.3°F] and 500 K [440.3°F] were included in the fit of Equation 41 in order to extend its temperature range).

THERMODYNAMIC TABLES AND DIAGRAMS

The preparation of tables of thermodynamic properties is a straightforward matter given a set of routines implementing an equation of state. A full set of FORTRAN property routines were developed for the MBWR equation of state based on the routines developed by Ely (1984). These routines computed reduced properties relative to the ideal gas reference state (e.g., $S(T, V)/R - S^o(T, V)/R$) and thus required modification to provide absolute quantities. The input and output format was also changed to yield a set of routines identical in form to those previously developed for the CSD equation of state (Morrison and McLinden 1985, 1986). Saturation properties, in both SI and inch-pound units, are presented as Tables 3 and 4. Space does not permit the presentation of a full set of superheated vapor properties; sample tables at atmospheric pressure (101.325 kPa [14.696 psia]) are given as Tables 5 and 6.

Diagrams of the thermodynamic properties on pressure-enthalpy and temperature-entropy coordinates were prepared as described by Gallagher et al. (1988). They are presented here as Figures 6–11.

SUMMARY AND DISCUSSION

Experimental measurements of the thermodynamic properties of two leading alternative refrigerants, R134a and R123, are described here. These measurements are particularly valuable in that a single group, working with common fluid samples, has carried out a diversified set of measurements. Where practical, the same property was measured on different apparatuses (e.g., vapor pressures on both the Burnett and variable-volume apparatus) as a consistency check. Additional checks were provided by complementary data (e.g., virial coefficients derived from both speed of sound and Burnett measurements).

These measurements, along with other data available in the literature, were used to fit a modified Benedict-Webb-Rubin equation of state, which, in turn, was used to generate tables and diagrams of the thermodynamic properties. This equation of state provides a consistent formulation of all the thermodynamic properties in the compressed liquid

Table 4b
Saturation Properties for R123; I-P Units

Temp (°F)	Pressure (psia)	Density (lb/ft^3) liq	Density (lb/ft^3) vap	Enthalpy (BTU/lb) liq	Enthalpy (BTU/lb) vap	Entropy (BTU/lb·°F) liq	Entropy (BTU/lb·°F) vap	C_v (BTU/lb·°F) liq	C_v (BTU/lb·°F) vap	C_p (BTU/lb·°F) liq	C_p (BTU/lb·°F) vap	σ (dyn/cm)	Temp (°F)
0.	2.0	97.8	0.06	8.2	87.6	0.018	0.190	0.160	0.138	0.202	0.152	20.7	0.
10.	2.6	97.0	0.08	10.2	89.0	0.022	0.190	0.161	0.140	0.205	0.155	20.0	10.
20.	3.5	96.2	0.11	12.3	90.4	0.026	0.189	0.162	0.142	0.209	0.157	19.3	20.
30.	4.5	95.4	0.13	14.4	91.8	0.031	0.189	0.163	0.145	0.213	0.160	18.6	30.
40.	5.8	94.6	0.17	16.6	93.3	0.035	0.189	0.163	0.147	0.218	0.162	17.9	40.
50.	7.3	93.7	0.21	18.8	94.7	0.040	0.189	0.164	0.149	0.222	0.165	17.2	50.
60.	9.2	92.9	0.26	21.0	96.2	0.044	0.189	0.165	0.151	0.226	0.167	16.5	60.
70.	11.4	92.0	0.32	23.3	97.7	0.048	0.189	0.166	0.153	0.231	0.170	15.9	70.
80.	14.1	91.1	0.39	25.6	99.1	0.053	0.189	0.167	0.155	0.235	0.172	15.2	80.
90.	17.2	90.3	0.47	28.0	100.6	0.057	0.189	0.168	0.157	0.240	0.174	14.5	90.
100.	20.8	89.4	0.56	30.4	102.1	0.061	0.189	0.169	0.159	0.244	0.177	13.9	100.
110.	25.0	88.4	0.66	32.9	103.5	0.066	0.190	0.170	0.161	0.248	0.179	13.2	110.
120.	29.8	87.5	0.79	35.4	105.0	0.070	0.190	0.171	0.162	0.252	0.181	12.6	120.
130.	35.3	86.5	0.92	37.9	106.5	0.074	0.191	0.171	0.164	0.256	0.183	12.0	130.
140.	41.5	85.6	1.08	40.5	107.9	0.079	0.191	0.172	0.165	0.259	0.185	11.3	140.
150.	48.5	84.6	1.26	43.1	109.3	0.083	0.192	0.173	0.167	0.263	0.188	10.7	150.
160.	56.5	83.6	1.46	45.8	110.7	0.087	0.192	0.173	0.168	0.265	0.190	10.1	160.
170.	65.3	82.5	1.68	48.5	112.1	0.091	0.193	0.174	0.169	0.268	0.193	9.5	170.
180.	75.2	81.5	1.93	51.2	113.5	0.096	0.193	0.175	0.170	0.271	0.195	8.9	180.
190.	86.1	80.4	2.21	53.9	114.8	0.100	0.194	0.175	0.171	0.273	0.198	8.3	190.
200.	98.2	79.2	2.52	56.6	116.1	0.104	0.194	0.176	0.172	0.275	0.201	7.7	200.
210.	111.5	78.1	2.87	59.4	117.3	0.108	0.195	0.176	0.173	0.277	0.205	7.1	210.
220.	126.1	76.9	3.26	62.1	118.5	0.112	0.195	0.177	0.174	0.279	0.208	6.5	220.
230.	142.1	75.6	3.69	64.9	119.7	0.116	0.196	0.177	0.175	0.281	0.213	6.0	230.
240.	159.4	74.3	4.18	67.7	120.8	0.120	0.196	0.177	0.177	0.283	0.218	5.4	240.
250.	178.3	73.0	4.72	70.6	121.8	0.124	0.196	0.178	0.178	0.285	0.224	4.8	250.
260.	198.8	71.5	5.33	73.4	122.8	0.128	0.197	0.178	0.179	0.288	0.232	4.3	260.
270.	221.1	70.0	6.01	76.3	123.7	0.132	0.197	0.179	0.181	0.292	0.241	3.8	270.
280.	245.1	68.4	6.78	79.1	124.5	0.136	0.197	0.180	0.183	0.297	0.252	3.3	280.
290.	271.0	66.7	7.66	82.1	125.3	0.140	0.197	0.181	0.186	0.304	0.266	2.8	290.
300.	299.0	64.9	8.67	85.0	125.9	0.143	0.197	0.182	0.189	0.313	0.283	2.3	300.
310.	329.2	62.9	9.83	88.1	126.4	0.147	0.197	0.184	0.193	0.325	0.306	1.9	310.
320.	361.8	60.9	11.19	91.2	126.8	0.151	0.197	0.187	0.197	0.343	0.337	1.4	320.
330.	397.0	58.6	12.79	94.4	127.0	0.155	0.196	0.190	0.203	0.371	0.380	1.0	330.
340.	435.0	56.1	14.73	97.8	127.1	0.159	0.196	0.195	0.210	0.421	0.446	0.7	340.
350.	476.0	53.0	17.19	101.6	126.8	0.164	0.195	0.200	0.218	0.527	0.575	0.3	350.

and superheated vapor regions, as well as for saturated conditions. The maximum pressure for this formulation is 10,000 kPa (1500 psia); the applicable temperature range is 233 to 450 K (−40° to 350°F) for R134a and 255 to 450 K (0° to 350°F) for R123.

The R123 results presented here are for isomerically pure 1,1-dichloro-2,2,2-trifluoroethane ($CHCl_2CF_3$). The eventual commercial product is likely to contain a significant (approximately 5%–10%) quantity of the isomer R123a (1,2-dichloro-1,2,2-trifluoroethane; $CHClFCClF_2$). The limited data on R123a suggest that it is unlikely that the properties of R123 and R123a differ significantly. (For example, the boiling points of the two isomers differ by less than 2.1 K (3.9°F).) Thus, the formulation presented here for isomerically pure R123 should also apply to R123/R123a mixtures. The impact of R123a on the properties of "R123" remains an area for future work. Apart from the lack of data for R123a, it is not feasible to prepare a lasting set of tables and diagrams for the R123/R123a mixture at this time because the R123a content of commercial grade R123 is highly dependent on process conditions employed in its production, conditions that are currently in a state of flux as the processes are refined.

While the formulations presented here cover the full range of conditions of interest for refrigeration applications and are based on a modern, well-proven equation of state, and while they are felt to represent the best possible formulation with the available data, they cannot be considered as final. As discussed above, the compressed liquid region is based on estimation methods. But perhaps the most pressing need is for calorimetric (e.g., heat capacity) information for the liquid phase and for the vapor phase at pressures higher than those covered by the sound speed measurements. The calculation of heat capacity requires the evaluation of first and second derivatives of the equation of state, so that any errors in p-V-T or other data are greatly magnified. Heat capacity data are thus an excellent check on the entire thermodynamic surface. Work continues on such measurements, both on the fluids considered here and on additional promising alternative working fluids.

Apart from the thermodynamic properties, knowledge of the transport properties (e.g., viscosity, thermal conductivity) is needed, particularly for equipment design. Again, additonal work is under way to collect these vital data.

Table 5a
Superheated Vapor Properties for R134a; SI Units

Pressure = 101.325 kPa

Temp (°C)	Density (kg/m³)	Enthalpy (kJ/kg)	Entropy ------	C_v (kJ/kg·K)	C_p -----	u (m/s)
-26.1*	1373.16	16.2	0.067	0.741	1.197	
-26.1+	5.26	232.0	0.941	0.682	0.787	145.7
-25.0	5.23	232.9	0.944	0.684	0.788	146.1
-20.0	5.11	236.8	0.960	0.691	0.794	147.8
-15.0	5.00	240.8	0.976	0.699	0.799	149.4
-10.0	4.89	244.8	0.991	0.706	0.805	151.0
-5.0	4.79	248.9	1.006	0.714	0.811	152.6
0.0	4.69	252.9	1.021	0.722	0.818	154.2
5.0	4.59	257.0	1.036	0.730	0.825	155.7
10.0	4.50	261.2	1.051	0.738	0.831	157.2
15.0	4.42	265.3	1.066	0.746	0.838	158.7
20.0	4.34	269.6	1.080	0.754	0.846	160.1
25.0	4.26	273.8	1.095	0.762	0.853	161.5
30.0	4.18	278.1	1.109	0.770	0.860	162.9
35.0	4.11	282.4	1.123	0.778	0.867	164.3
40.0	4.04	286.8	1.137	0.786	0.875	165.7
45.0	3.97	291.1	1.151	0.793	0.882	167.0
50.0	3.91	295.6	1.165	0.801	0.890	168.4
55.0	3.84	300.0	1.178	0.809	0.897	169.7
60.0	3.78	304.6	1.192	0.817	0.905	171.0
65.0	3.73	309.1	1.206	0.825	0.912	172.3
70.0	3.67	313.7	1.219	0.833	0.920	173.6
75.0	3.61	318.3	1.232	0.841	0.927	174.8
80.0	3.56	322.9	1.246	0.849	0.935	176.1

* saturated liquid
+ saturated vapor

Table 5b
Superheated Vapor Properties for R134a; I-P Units

Pressure = 14.70 psia

Temp (°F)	Density (lb/ft³)	Enthalpy (BTU/lb)	Entropy ----	C_v (BTU/lb·°F)	C_p ---	u (ft/s)
-15.0*	85.723	7.0	0.016	0.177	0.286	
-15.0+	0.329	99.8	0.225	0.163	0.188	478.0
-10.0	0.324	100.7	0.227	0.164	0.189	481.1
0.0	0.316	102.6	0.231	0.166	0.190	487.2
10.0	0.308	104.6	0.235	0.168	0.192	493.2
20.0	0.301	106.5	0.239	0.170	0.193	499.0
30.0	0.294	108.4	0.243	0.172	0.195	504.7
40.0	0.287	110.4	0.247	0.174	0.197	510.3
50.0	0.281	112.4	0.251	0.176	0.199	515.7
60.0	0.275	114.4	0.255	0.178	0.201	521.1
70.0	0.270	116.4	0.259	0.181	0.202	526.3
80.0	0.264	118.4	0.263	0.183	0.204	531.5
90.0	0.259	120.5	0.267	0.185	0.206	536.6
100.0	0.254	122.5	0.270	0.187	0.208	541.6
110.0	0.249	124.6	0.274	0.189	0.210	546.5
120.0	0.245	126.7	0.278	0.191	0.212	551.4
130.0	0.240	128.9	0.281	0.193	0.214	556.2
140.0	0.236	131.0	0.285	0.195	0.216	561.0
150.0	0.232	133.2	0.288	0.197	0.218	565.7
160.0	0.228	135.4	0.292	0.200	0.220	570.4
170.0	0.224	137.6	0.296	0.202	0.222	575.0
180.0	0.221	139.8	0.299	0.204	0.224	579.5
190.0	0.217	142.1	0.303	0.206	0.226	584.0
200.0	0.214	144.4	0.306	0.208	0.228	588.5

* saturated liquid
+ saturated vapor

Table 6a
Superheated Vapor Properties for R123; SI Units

Pressure = 101.325 kPa

Temp (°C)	Density (kg/m³)	Enthalpy (kJ/kg)	Entropy ------	C_v (kJ/kg·K)	C_p -----	u (m/s)
27.9*	1456.95	60.8	0.224	0.700	0.988	
27.9+	6.47	231.2	0.790	0.652	0.722	128.8
30.0	6.41	232.7	0.795	0.652	0.721	129.3
35.0	6.29	236.3	0.807	0.654	0.721	130.6
40.0	6.18	239.9	0.819	0.655	0.721	131.8
45.0	6.06	243.5	0.830	0.658	0.723	133.0
50.0	5.96	247.1	0.841	0.660	0.724	134.2
55.0	5.86	250.8	0.852	0.664	0.727	135.4
60.0	5.76	254.4	0.863	0.667	0.729	136.6
65.0	5.67	258.0	0.874	0.671	0.732	137.7
70.0	5.58	261.7	0.885	0.674	0.736	138.9
75.0	5.49	265.4	0.896	0.678	0.739	140.0
80.0	5.41	269.1	0.906	0.683	0.743	141.1
85.0	5.32	272.8	0.917	0.687	0.747	142.2
90.0	5.25	276.6	0.927	0.691	0.751	143.3
95.0	5.17	280.3	0.937	0.696	0.756	144.3
100.0	5.10	284.1	0.948	0.700	0.760	145.4
105.0	5.02	287.9	0.958	0.705	0.764	146.4
110.0	4.95	291.8	0.968	0.710	0.769	147.5
115.0	4.89	295.6	0.978	0.714	0.774	148.5
120.0	4.82	299.5	0.988	0.719	0.778	149.5

* saturated liquid
+ saturated vapor

Table 6b
Superheated Vapor Properties for R123; I-P Units

Pressure = 14.70 psia

Temp (°F)	Density (lb/ft³)	Enthalpy (BTU/lb)	Entropy ----	C_v (BTU/lb·°F)	C_p ---	u (ft/s)
82.2*	90.954	26.1	0.054	0.167	0.236	
82.2+	0.404	99.4	0.189	0.156	0.173	422.4
90.0	0.397	100.8	0.191	0.156	0.172	426.1
100.0	0.389	102.5	0.194	0.156	0.172	430.7
110.0	0.381	104.2	0.197	0.157	0.173	435.2
120.0	0.374	106.0	0.200	0.158	0.173	439.6
130.0	0.366	107.7	0.203	0.159	0.174	443.9
140.0	0.360	109.4	0.206	0.159	0.174	448.1
150.0	0.353	111.2	0.209	0.160	0.175	452.3
160.0	0.347	112.9	0.212	0.161	0.176	456.4
170.0	0.341	114.7	0.215	0.162	0.177	460.5
180.0	0.335	116.5	0.218	0.164	0.178	464.5
190.0	0.330	118.3	0.221	0.165	0.179	468.4
200.0	0.324	120.1	0.223	0.166	0.180	472.4
210.0	0.319	121.9	0.226	0.167	0.181	476.2
220.0	0.314	123.7	0.229	0.168	0.183	480.1
230.0	0.309	125.5	0.231	0.170	0.184	483.9
240.0	0.305	127.4	0.234	0.171	0.185	487.6
250.0	0.300	129.2	0.237	0.172	0.186	491.4
260.0	0.296	131.1	0.239	0.173	0.187	495.1
270.0	0.291	133.0	0.242	0.175	0.189	498.7

* saturated liquid
+ saturated vapor

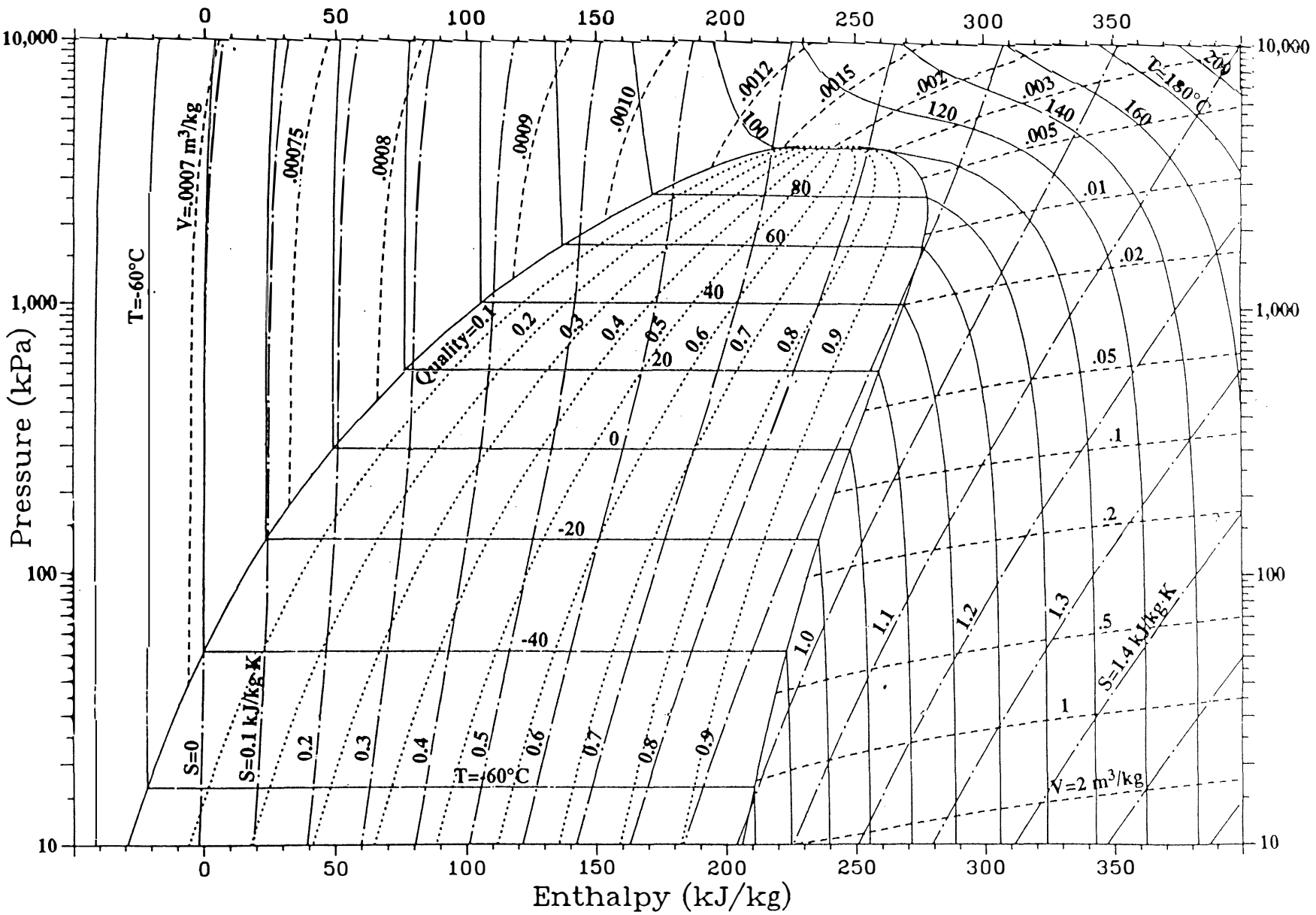

Figure 6 *Thermodynamic properties of R134a, SI units*

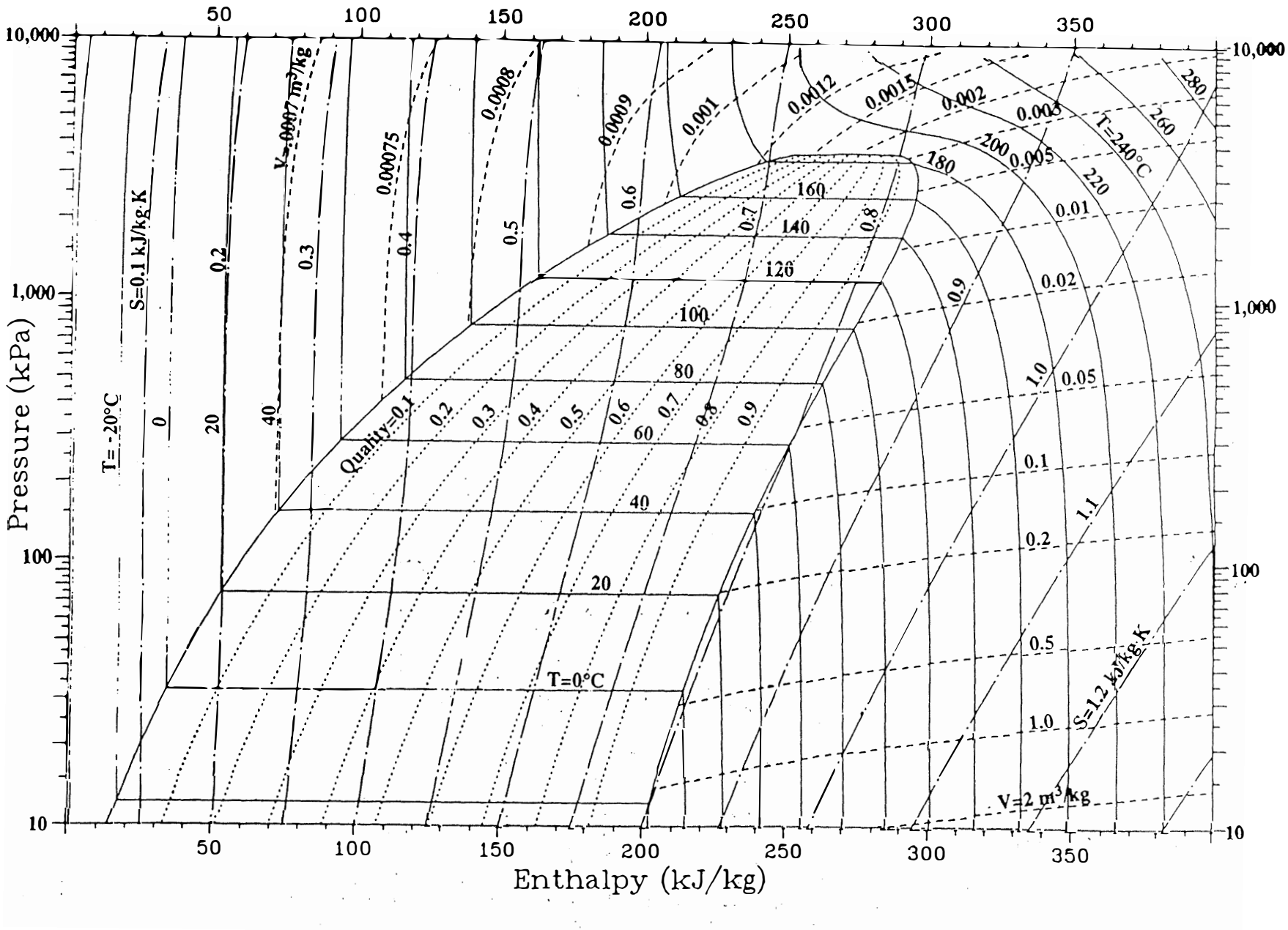

Figure 7 Thermodynamic properties of R123, SI units

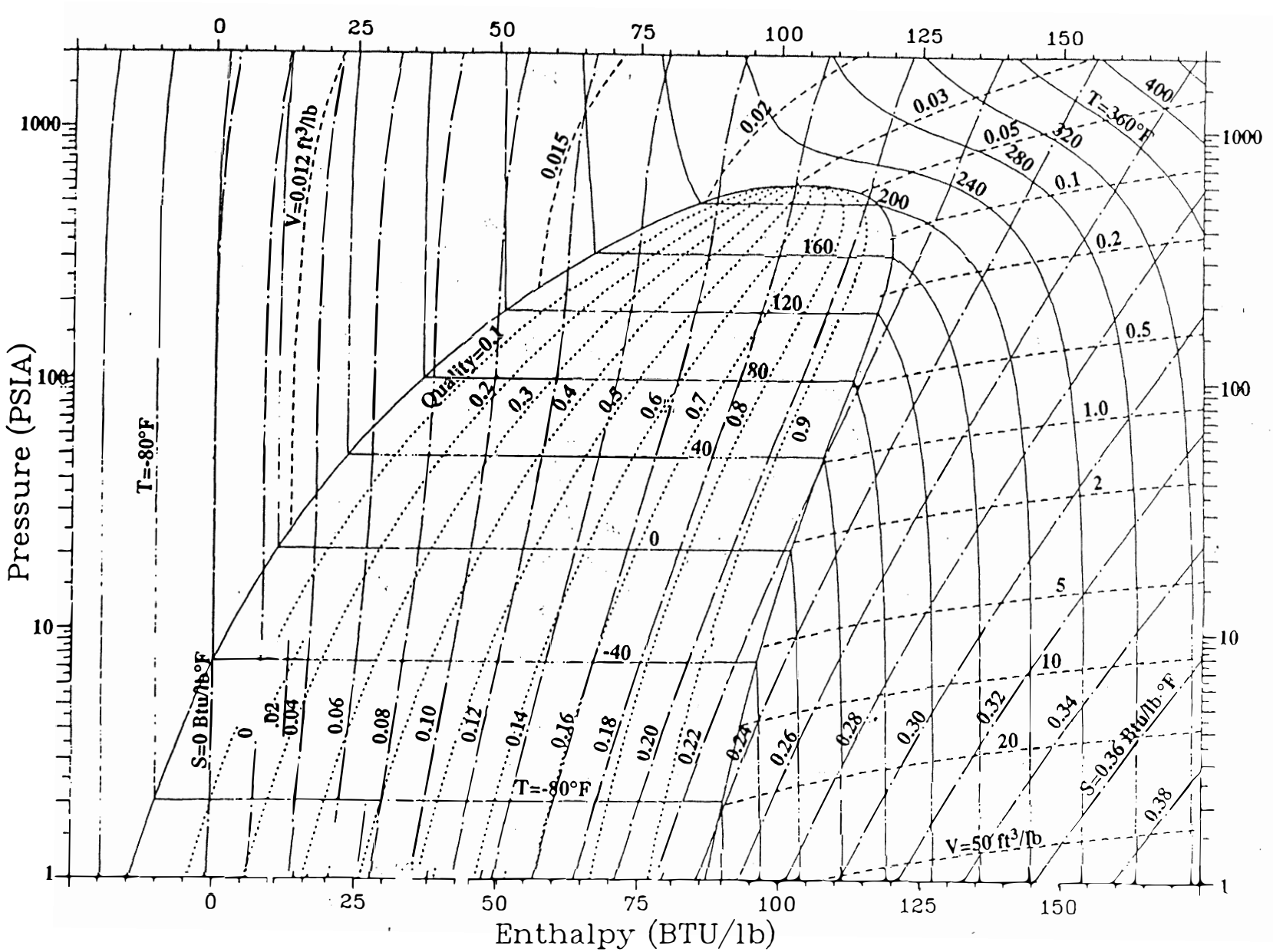

Figure 8 *Thermodynamic properties of R134a, English units*

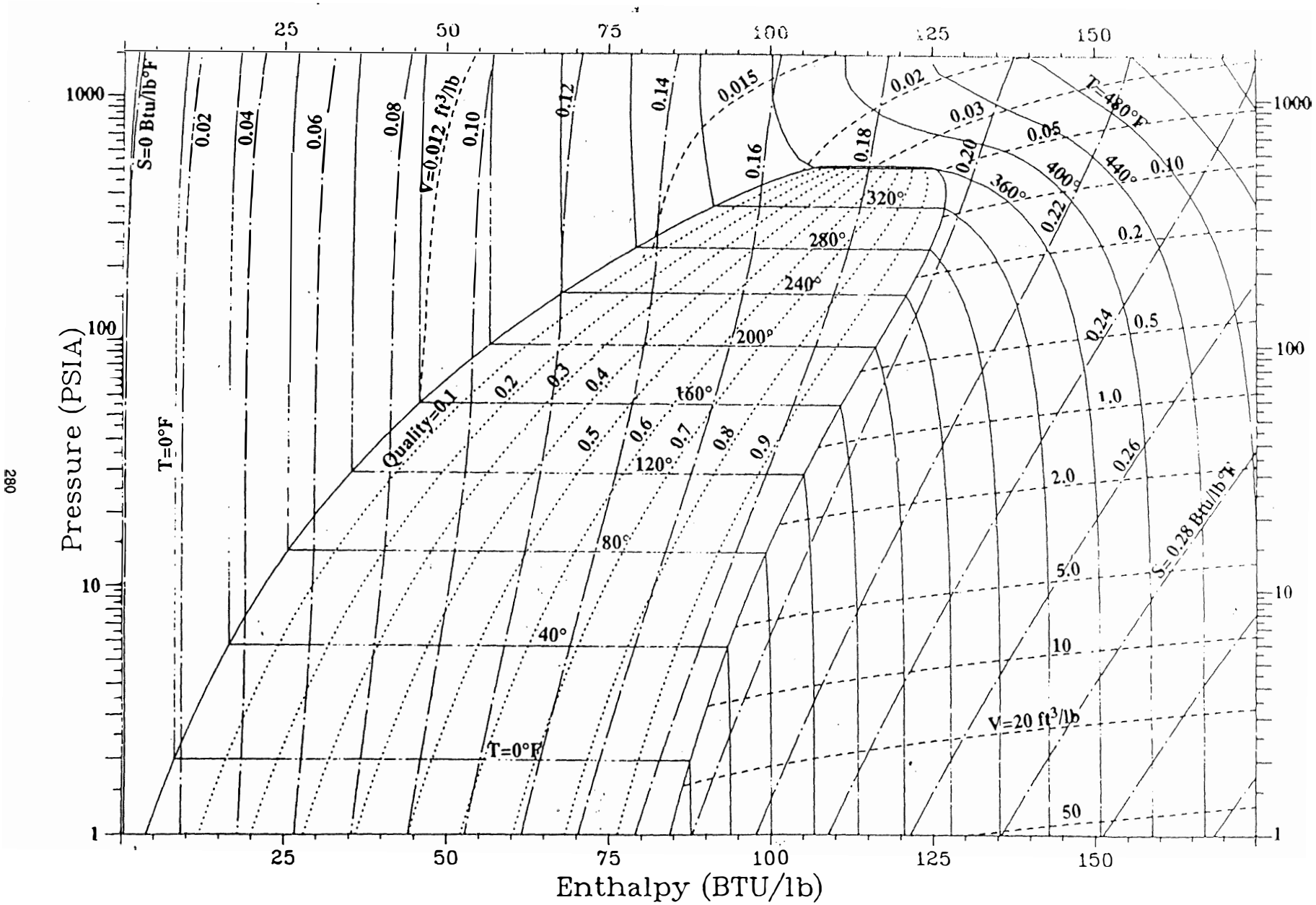

Figure 9 *Thermodynamic properties of R123, English units*

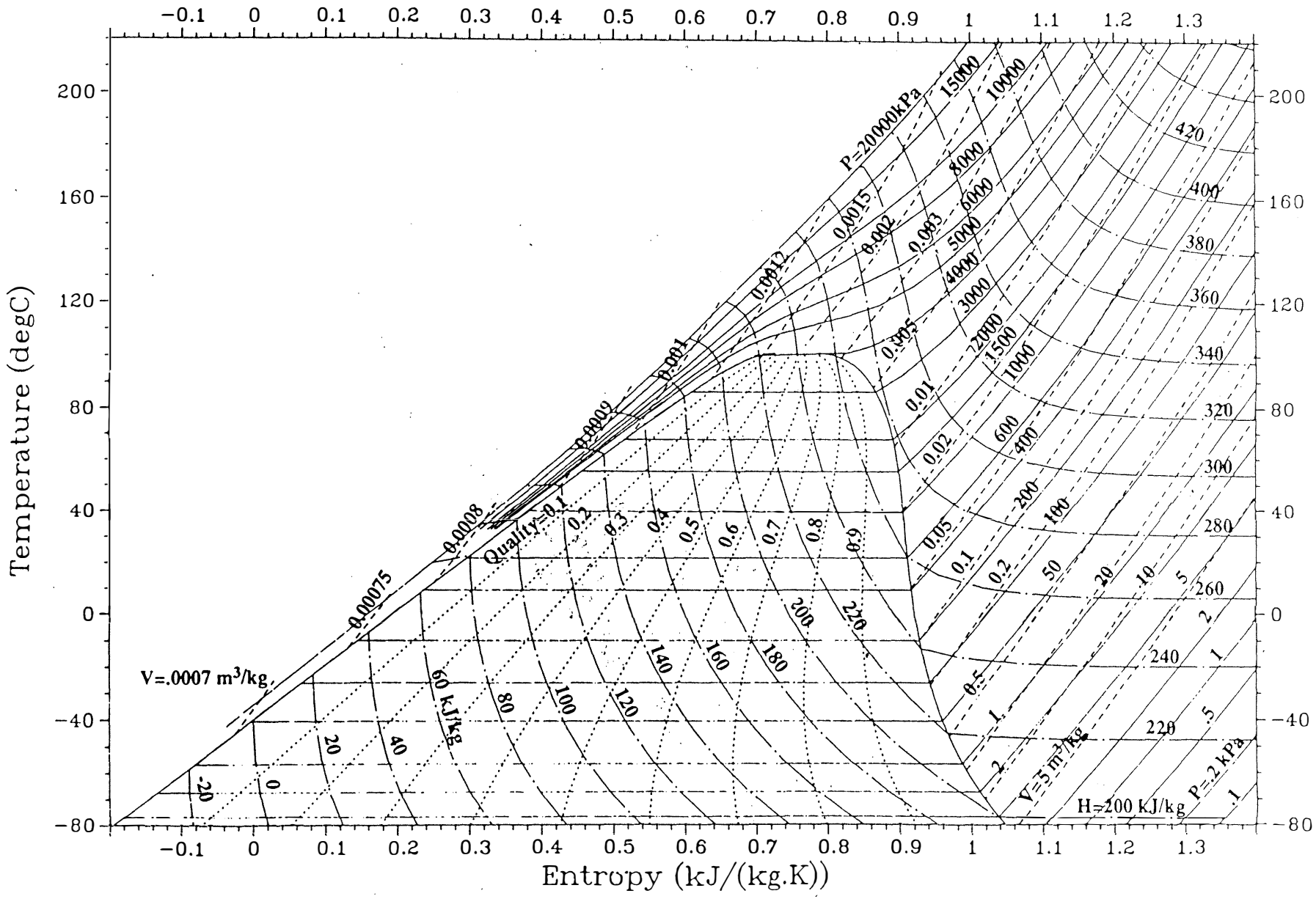

Figure 10 Thermodynamic properties of R134a on temperature-entropy coordinates

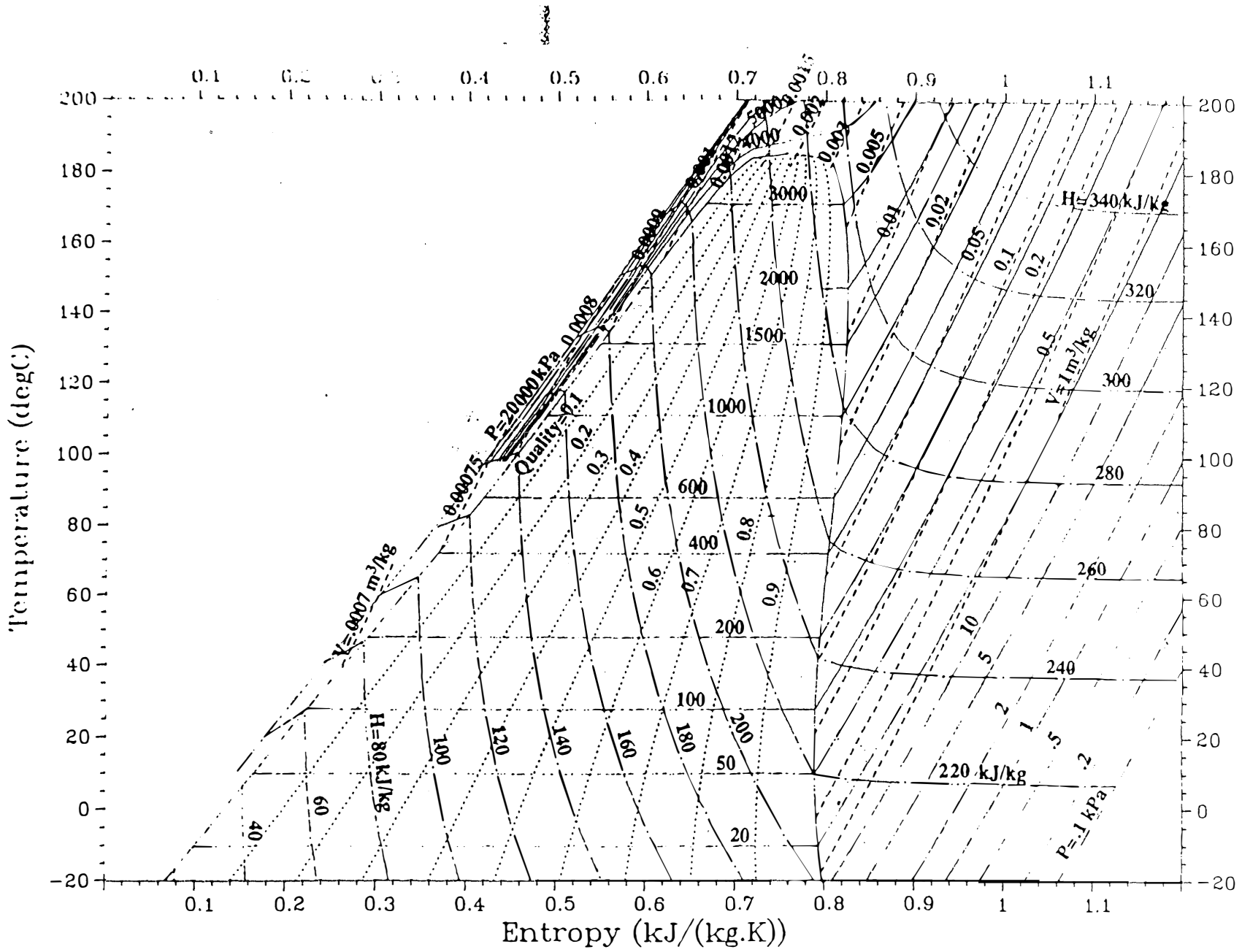

Figure 11 *Thermodynamic properties of R123 on temperature-entropy coordinates*

ACKNOWLEDGMENTS

This work was supported by the National Institute of Standards and Technology, the Office of Building and Community Systems of the U.S. Department of Energy, the Global Change Division of the U.S. Environmental Protection Agency, and the American Society of Heating, Refrigerating, and Air-Conditioning Engineers (RP-588 under the sponsorship of TC 3.1, Refrigerants and Brines). We also gratefully acknowledge the donation of fluid samples from E. I. duPont de Nemours and Company, Inc., and Allied-Signal.

REFERENCES

ASHRAE. 1986. "ASHRAE thermodynamic properties of refrigerants." Atlanta: American Society of Heating, Refrigerating, and Air-Conditioning Engineers, Inc.

Burnett, E.J. 1936. *Journal of applied mechanics*, Vol. 3, p. 136.

Carnahan, N.F., and Starling, K.E. 1969. "Equation of state for nonattracting rigid spheres." *Journal of Chemical Physics*, Vol. 51, No. 2, pp. 635-636.

Chaar, H.; Moldover, M.R.; and Schmidt, J.W. 1986. "Universal amplitude ratios and the interfacial tension near consulate points of binary liquid mixtures." *Journal of Chemical Physics*, Vol. 85, pp. 418-247.

Chae, H.B.; Schmidt, J.W.; and Moldover, M.R. 1989. "Surface tension of refrigerants R123 and R134a." Manuscript submitted to *Journal of Chemical and Engineering Data*.

Chen, S.S.; Rodgers, A.S.; Chao, J.; Wilhoit, R.S.; and Zwolinski, B.J. 1975. "Ideal gas thermodynamic properties of six fluoroethanes." *Journal of Physical and Chemical Reference Data* Vol. 4, pp. 441-456.

Davis, H.A. 1983. "Low-cost tubular sapphire optical cells for study of phase separation in fluid mixtures." *Review of Scientific Instruments* Vol. 54, p. 1412.

DeSantis, R.; Gironi, F.; and Marrelli, L. 1976. "Vapor-liquid equilibrium from a hard-sphere equation of state." *Industrial and Engineering Chemistry, Fundamentals* Vol. 15, No. 3, pp. 183-189.

Ely, J.F. 1984. "Application of the extended corresponding states model to hydrocarbon mixtures." Proceedings, 63rd Gas Processors Association Annual Convention, New Orleans, pp. 9-22.

Ewing, M.B.; Goodwin, A.R.H.; McGlashan, M.L.; and Trusler, J.P.M. 1988. "Thermophysical properties of alkanes from speeds of sound determined using a spherical resonator 2. n-butane." *Journal of Chemical Thermodynamics* Vol. 20, pp. 243-256.

Gallagher, J.S.; McLinden, M.O.; and Morrison, G. 1988. "Thermodynamic diagrams for refrigerant mixtures." *ASHRAE Transactions*, Vol. 94, Part 2, pp. 2119-2136.

Goodwin, A.R.H., and Moldover, M.R. 1989. Manuscript in preparation.

Hickman, K. 1988. York International Corporation, York, PA, personal communication.

Hocken, R.; Moldover, M.R.; Muth, E.; and Gerner, S. 1975. "Versatile cells for optical studies in fluids." *Review of Scientific Instruments*, Vol. 46, p. 1699.

Jacobsen, R.T., and Stewart, R.B. 1973. "Thermodynamic properties of nitrogen including liquid and vapor phases from 63 K to 2000 K with pressures to 10,000 bar." *Journal of Physical and Chemical Reference Data*, Vol. 2, pp. 757-922.

Kabata, Y.; Tanikawa, S.; Uematsu, M.; and Watanabe, K. 1988. "Measurements of the vapor-liquid coexistence curve and the critical parameters for 1,1,1,2-tetrafluoroethane." *International Journal of Thermophysics*, Vol. 10, No. 3, pp. 605-615.

Linsky, D.; Levelt-Sengers, J.M.H.; and Davis, H.A. 1987. "Semiautomated PVT facility for fluids and fluid mixtures." *Review of Scientific Instruments*, Vol. 58, pp. 817-821.

Luft, N.W. 1954. "Assignment of torsional frequencies in some halogenated ethanes." *Journal of Chemical Physics*, Vol. 22, pp. 155-156.

McCarty, R.D. 1980. "Interactive FORTRAN IV computer programs for the thermodynamic and transport properties of selected cryogens (fluids pack)." NBS Technical Note 1025 National Bureau of Standards, Gaithersburg, MD.

Mehl, J.B., and Moldover, M.R. 1981. "Precision acoustic measurements with a spherical resonator: Ar, C_2H_4." *Journal of Chemical Physics* Vol. 74, p. 4062.

Moldover, M.R.; Waxman, M.; and Greenspan, M. 1979. "Spherical acoustic resonators for temperature and thermophysical property measurements." *High Temperature and High Pressure*, Vol. 11, pp. 75-86.

Morrison, G., and Kincaid, J.M. 1984. "Critical point measurements on nearly polydisperse fluids." *AIChE Journal*, Vol. 30, p. 257.

Morrison, G., and McLinden, M.O. 1985. "Application of a hard sphere equation of state to refrigerants and refrigerant mixtures." NBS Technical Note 1226. National Bureau of Standards, Gaithersburg, MD.

Morrison, G., and McLinden, M.O. 1986. "Application of the Carnahan-Starling-DeSantis equation of state to mixtures of refrigerants." ASME Winter Annual Meeting, Anaheim, CA. paper 86-WA/HT-59.

Morrison, G., and Ward, D.A. 1989. "Saturation properties of two alternative refrigerants." Manuscript in preparation.

Rathjen, W., and Straub, H. 1973. Proceedings, International Institute of Refrigeration, Commission B1 Meeting. Zurich.

Rayleigh, O.M. 1916. Proceedings of the Royal Society of London, Series A 92, p. 184.

Waxman, M., and Hastings, J.R. 1971. *Journal of Research of the National Bureau of Standards*, Vol. 75C, nos. 3 and 4.

Weber, L.A. 1989. "Vapor pressures and gas phase PVT data for 1,1,1,2-tetra-fluoroethane." *International Journal of Thermophysics*, Vol. 10, No. 3, pp. 617-627.

Weber, L.A., and Levelt-Sengers, J.M.H. 1989. "Critical parameters and saturation densities of 1,1-dichloro-2,2,2-trifluoroethane." Accepted for publication in *Fluid Phase Equilibria*.

Wilson, D.P., and Basu, R.S. 1988. "Thermodynamic properties of a new stratospherically safe working fluid—refrigerant 134a." *ASHRAE Transactions*, Vol. 94, Part 2.

Younglove, B.A. 1982. "Thermophysical properties of fluids. I. Argon, ethylene, parahydrogen, nitrogen, nitrogen trifluoride, and oxygen." *Journal of Physical and Chemical Reference Data*, Vol. 11, supplement no. 1.

Younglove, B.A., and Ely, J.F. 1987. "Thermophysical properties of fluids. II. Methane, ethane, propane, isobutane and normal butane." *Journal of Physical and Chemical Reference Data*, Vol. 16, pp. 577-798.